NTNU

Norwegian University of
Science and Technology

Production Optimization in Shale Gas Reservoirs

Brage Rugstad Knudsen

Master of Science in Engineering Cybernetics
Submission date: June 2010
Supervisor: Bjarne Anton Foss, ITK

Norwegian University of Science and Technology
Department of Engineering Cybernetics

Problem Description

Extraction of natural gas from organic rich shales is challenging and complicated. The most prominent property of shale gas reservoirs is low permeability, and this is one of the reasons why shales are some of the last major sources of natural gas to be developed. However, shale can store enormous amounts of gas and may, by the use of modern recovery techniques, be very profitable.

Due to the low permeability, hydraulic fracturing is almost always performed at initial phases of the development of shale gas reservoirs. The gas production from the well will typically decrease rapidly, demanding regularly stimulation of the wells to maintain production. Several techniques exist for performing this stimulation. The most well-established technique is to apply the hydraulic fracturing on a regular basis. Another strategy is to switch between production and well shut-ins in a cyclic manner. Well shut-ins allow for recharging of fractures with gas and pressure build up in the stimulated regions of the reservoir. This second approach will be the focus of this master thesis, in particular assessing the potential of applying model-based optimization as a means to maximize production and long-term recovery.

The project includes the following tasks:
1.Finalize the development and validation of an appropriate model for wells in shale gas reservoirs.
2.Analyze production from one well using a cyclic production strategy.
3.Develop a system model for shale gas reservoirs which includes several wells as well as a suitable compression unit.
4.Formulate the production problem as an optimization problem. Both long-term recovery as well as short-term production planning should be included. Discuss alternative formulations and review literature as a background for the discussion.
5.Study the potential of using an optimization scheme and discuss the applicability of such a strategy in practice.

This master project will use the report Modeling and Simulation of Shale Gas Reservoirs written by the same candidate as its starting point.

Assignment given: 18. January 2010
Supervisor: Bjarne Anton Foss, ITK

Abstract

Natural gas from organic rich shales has become an important part of the supply of natural gas in the United States. Modern drilling and stimulation techniques have increased the potential and profitability of shale gas reserves that earlier were regarded as unprofitable resources of natural gas. The most prominent property of shale gas reservoirs is the low permeability. This is also the reason why recovery from shale gas wells is challenging and clarifies the need for stimulation with hydraulic fracturing. Shale gas wells typically exhibit a high initial peak in the production rate with a successive rapid decline followed by low production rates. Liquid accumulation is common in shale wells and is detrimental on the production rates.

Shut-ins of shale gas wells is used as a means to prevent liquid loading and boost the production. This strategy is used in a model-based production optimization of one and multiple shale gas well with the objective of maximizing the production and long-term recovery. The optimization problem is formulated using a simultaneous implementation of the reservoir model and the optimization problem, with binary variables to model on/off valves and an imposed minimal production rate to prevent liquid loading. A reformulation of the nonlinear well model is applied to transform the problem from a mixed integer nonlinear program to a mixed integer *linear* program.

Four numerical examples are presented to review the potential of using model-based optimization on shale gas wells. The use of shut-ins with variable duration is observed to result in minimal loss of cumulative production on the long term recovery. For short term production planning, a set of optimal production settings are solved for multiple wells with global constraints on the production rate and on the switching capacity. The reformulation to a mixed integer linear program is shown to be effective on the formulated optimization problems and allows for assessment of the error bounds of the solution.

Preface

This master thesis is written during the last semester of the five year Master of Science program in Engineering Cybernetics at the Norwegian University of Science and Technology.

The background of this thesis is the growing interest in exploration of shale gas reservoirs, involving extensive challenges in production and recovery techniques. I have enjoyed working with this thesis, acquiring new knowledge of both petrophysics, operation research and mixed integer programming.

I would like to thank my supervisor Professor Bjarne A. Foss for constructive and encouraging discussions on the master thesis. The support on the reservoir modeling from Professor Curtis H. Whitson at the Department of Petroleum Engineering and Applied Geophysics is gratefully appreciated. A special thanks goes to PhD candidate Vidar Gunnerud for the time he has devoted on discussions on the formulation and implementation of the optimization problems. I would also like to thank the fellow students at the Department of Engineering Cybernetics for providing a rewarding and supporting working environment, and my girlfriend Sigrid for her support during this master thesis.

Trondheim, June 21, 2010
Brage Rugstad Knudsen

Contents

Chapter 1

Introduction

As an introduction to production of shale gas, this chapter gives a brief summary of the geological and physical properties of shale gas and the motivation for recovery of gas from shale gas reservoirs. Emphasis is put on the challenges associated with recovery of gas from the tight shale rock. The use of shale gas is seen in context of other unconventional gas resources, and a review of today's level of shale gas production is included.

This chapter is based on the introductory chapter in Knudsen (2010).

1.1 Background

Extraction of natural gas from sources of organic rich, tight shales is inherently challenging. Traditionally, shale gas wells have only been marginally profitable, and this is also why shales is one last major resource of natural gas to be developed. With extensive developments of drilling and stimulation techniques over the last decade, the substantial asset and potential in shale gas have been highlighted. This has generated significant interest in the exploration of shale gas in several European countries, and particularly in China. The United States are the world leader on shale gas recovery and are the driving force behind the last decade's vast developments in this industry.

Shale gas is one out of several types of *unconventional gas* resources. Tight gas and coalbed methane are two other sources of developed unconventional gas resources, both with the property of the gas being stored in tight formations. However, shale is far tighter and less permeable than these two categories of unconventional gas resource. This is one of the reasons why the production of shale gas has been lower compared to the production these

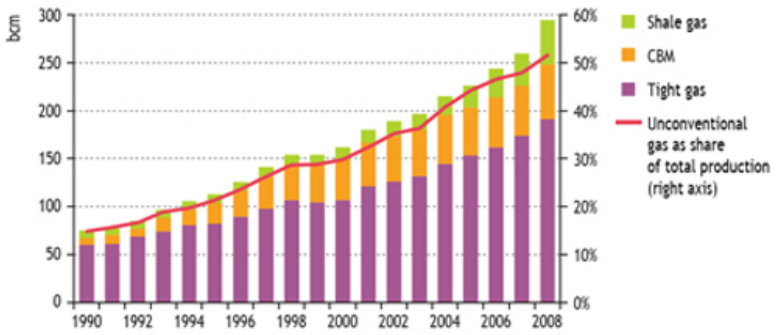

Figure 1.1: Production of unconventional gas in the United States from 1990 to 2008. Source: WEO (2009), data from by the US Department of Energy/Energy Information Administration.

types of unconventional gas. This is seen in figure 1.1 of the production of unconventional gas in the United States WEO (2009). The same figure also shows the substantial increase in the production of shale gas in the United States since year 2000. The gas in shales is stored by different mechanisms: some is stored within the pores and small natural systems of fractured of the rock, while much of the gas is absorbed on the surface of the shale itself or dissolved in organic content(Carlson and Mercer, 1991; Carlson, 1994). Hence the storage mechanisms of shales are substantially different from conventional reservoirs, where the gas is stored in relatively large open pores with a geological trap to hold the gas in place. The organic richness of shales depends heavily on geological location and how the gas content in the shale was created. Far from all of the discovered shale gas resources are economically profitable with today's recovery techniques.

The discussion and presentation of the shale gas characteristics and developments will be based on the shale gas production in the United States, as this shale gas industry is by far the most developed and well documented. Figure 1.2 gives an overview of the known shale gas resources in the lower states of the U.S. The most famous and developed shale formations are the Barnett Shale in Texas and the Devonian Shale in eastern U.S. Other famous shale gas locations include Haynesville, Fayetteville, Marcellous and Woodford. Only considering the shale gas resources in the U.S., these are estimated to be between 500 and 1000 trillion cubic feet (Arthur et al., 2008). The US Energy Information Administration reported a yearly shale gas production of 1,184 bcf (billion cubic feet) in 2007 and 2,022 bcf in 2008.

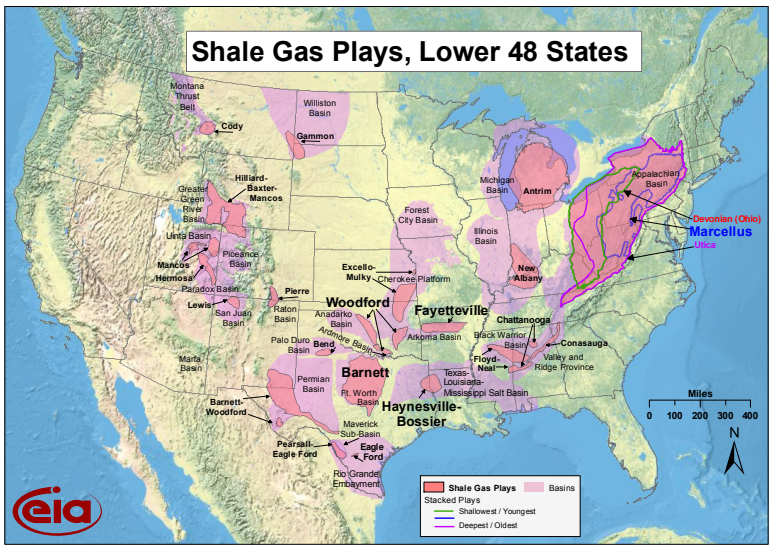

Source: Energy Information Administration based on data from various published studies.
Updated: March 10, 2010

Figure 1.2: Map of the shale gas resources in the U.S as of May 2009. Source: *Energy Information Administration*

The report *World Energy Outlook 2009* by the International Energy Agency WEO (2009) describes natural gas a resource for building a bridge from the current extensive use of fossil-fuel in energy production to cleaner and renewable energy in the future. This as gas-fired power plants are considered to be more environmental friendly than coal-based power generation (WEO, 2009). Unconventional gas developments and in particular the shale gas developments may therefore provide large resources of natural gas to gradually replace the extensive use of coal in power generation.

1.2 Shale gas characteristics

The shale is generally too tight for the gas to flow directly from the storage in the rock to the well. While in conventional gas reservoirs where large amounts of gas flow directly from the storage pores to the well, these quantities will only last in the scale of *minutes* in shale gas reservoirs (Carlson and Mercer, 1991). The gas in shales mainly consists of methane. Due to the tightness of the shale, the gas will only travel a very short distance in the rock over a given reasonable time span. Schettler et al. (1989) and Carlson (1994) describes this flow through the rock itself predominately as a result of molecular diffusion. The majority of the gas flow in shales arises from the

molecules traveling the short distance from the storage in the tight rock to adjacent segments of fractures in the rock itself. The rock in this context describes a piece of tight shale rock. The gas then flows from these small segments of fractures to larger networks of fractures in the shale. This physical process makes the gas flow in shale gas reservoirs examples of *dual porosity* behavior.

The key characteristic of shale gas reservoirs is the low permeability. Permeability is a measure of a materials' ability to transmit fluids, in this context the shales ability to transmit the gas. For shale gas reservoirs, the effective permeability may often be in the range of 10^{-3} mD to 10^{-6} mD. This emphasize the difficulties and challenges of recovering gas from shales compared to conventional viscous reservoirs. Many factors impact the gas production from shale gas reservoirs, where the most prominent is the number and the structural complexity of fracture network (Cipolla, 2009). The effective conductivity of fractures and the actual permeability of the shale rock are also crucial for the productivity.

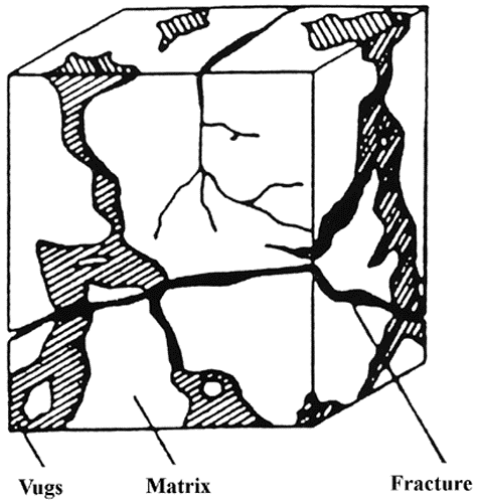

Figure 1.3: Illustration of the mechanisms in the gas flow in shales. From Warren and Root (1963)

Shale gas reservoirs are essentially land-based. A typical developed shale gas play[1] consist of a large number of wells. The geological properties of shale gas reservoirs vary widely between the shale gas plays. Many of the geological properties are hard to identify or estimate, and for some only the span

[1]The established expression in the literature used to describe a shale gas area

of the parameter value can be quantified. The reservoir permeability is by far the most difficult parameter to predict. It is also the most dominating property for the productivity of shale gas, thereby causing unpredictability in the production forecast and uncertainty in reservoir simulations. North (1990) describes the typical permeability of shale rock to be in the range of $5 \cdot 10^{-2}$ - $1 \cdot 10^{-5}$ mD, which agrees with the values given in Smith (2007) for Barnett shale. Shale gas reservoirs are typical found on depth ranging from 300 to 4000 meters (1000 to 13000 ft), with net thickness ranging from 15 to 183 meters (50 to 600 ft) (Cipolla et al., 2009). The porosity is normally in the range 2-8% and the amount of total organic content is 1 to 14%.

The Newark East field in Northeast Texas - referred to as the Barnett Shale - is currently the most active shale gas play in the United States (WEO, 2009). Using the average properties of these wells thus serve as a good basis for the simulations. As an example of shale gas reservoir properties, the average properties of the Barnett Shale is shown in table 1.1. The data are compiled from the sources Cipolla et al. (2009); Jenkins and Boyer II (2008); J.H. Frantz, Jr. et al. (2005); Smith (2007); WEO (2009). The entries in table 1.1 are somewhat spread out in the different sources, but they give a hint of the actual respective reservoir properties.

Table 1.1: Average reservoir properties in Barnett Shale reservoirs

Reservoir depth	2000-2600 meters
Reservoir thickness	30-200 meters
Porosity	4-5%
Permeability	$9 \cdot 10^{-6}$ - $5 \cdot 10^{-3}$ mD
Total organic content	4.5%
Basin size	13 000 km^2
Number of producing wells in 2008	12 000
Gas rate per well	100-3000 mcf per day
Recovery factor	5-20 %
Total annual production	$44 \cdot 10^9\ \mathrm{m}^3$

1.3 Recovery techniques

The properties of a shale gas reservoir requires new and challenging recovery techniques compared to those used in conventional oil and gas reservoirs.

Based on the above description of these reservoirs, the key to high production rates is to maximize the area of the reservoir exposed to the network of fractures connected to the wellbore. The standard technique used to stimulate the network of fractures is known as *hydraulic fracturing*. Large volumes of water with specially designed proppant is pumped into the reservoir at high rates and pressure, stimulating and extending the small existing fractures in the shale rock. This creates conduits of high conductivity and variable size, leading the gas to the wellbore. The proppant is used to prevent the new fractures from closing, and often consists of grains of sand. The fractures created are large and complex, and are stretching in both horizontal and vertical direction. Hydraulic fracturing is normally performed in multiple stages, and is a well established technique for stimulating horizontal wells in tight gas formations (Medeiros et al., 2007). Most of the currently exploited shale gas resources are developed with horizontal wells (Cipolla, 2009), but the technique is also applicable to vertical wells.

Due to the low permeability, hydraulic fracturing is almost always performed at initial phases of the development of shale gas reservoirs. The gas production from the well will typically decrease very rapidly, demanding regularly stimulation of the wells to maintain production. Two more or less established techniques exist for stimulation of the wells. The most well-established technique is to apply the hydraulic fracturing on a regular basis, which is an expensive but effective technique to preserve the production from shale gas wells. Another strategy for maintaining the production, is to alternate the production and shut-ins in a cyclic manner. Depending on the shut-in interval and time, this allows for recharging of fractures with gas and pressure build up in the stimulated regions of the reservoir. This approach is described in Rahmawati et al. (2009), where the production from a single well in a tight gas reservoir was optimized using a constant shut-in period.

Liquid accumulation in the well is a prominent problem for shale gas wells, and is one of the key factors for the rapid fall in production of gas. The liquid accumulation may cause the phenomenon known as *liquid loading*, a state of the well where the backpressure on the well is high on the gas rate is erratic and unpredictable. It is important to address this problem as the well eventually will die. The preferred technology by many operators to address this problem, in particular operators of Barnett shale, is the use of gas lift (Elmer et al., 2009). The use of gas lift is an effective method for decreasing the backpressure on the well resulting from the liquid accumulation, while the drawback is the necessary source of lift-gas. Another strategy to prevent liquid loading is to apply regularly shut-ins of the well with variable

duration, allowing for pressure build-up in the well and thus removal of the accumulated liquid. This particular strategy for accommodating liquid accumulation in the wells as well as boosting the production will be addressed in this report.

The available literature on production optimization of shale gas wells is limited. The focus in the literature is mainly on the complex modeling of the fracture network and stimulation technique with hydraulic water. Production optimization applied to conventional petroleum reservoirs and similar applications is therefore studied and used partly as background for the study in this report.

1.4 Scope

The scope of this master thesis is to study the potential of applying model-based production optimization in shale gas reservoirs. In particular, the idea is to apply shut-ins of the wells as a means to boost the production and prevent liquid loading in the wells. The intention is further to assess how such a production strategy may be used to maximize the gas production and long-term recovery from one and several shale gas wells as an alternative or supplement to performing stimulation with hydraulic fracturing on a regular basis.

1.5 Report outline

This report is organized as follows:

- Chapter 2 presents the reservoir modeling, with reservoir simulations and model discussion in chapter 3.
- In chapter 4, the derivation of the production optimization problems is described.
- Chapter 5 describes the different implementations and solution approaches used to solve the optimization problems in chapter 4. This chapter also includes a review of alternative problem formulations.
- Chapter 6 presents four numerical examples of shale gas production optimization, with discussion of the results and the practical applicability in chapter 7.

Chapter 2

Reservoir and well modeling

This section describes the reservoir and well model used to describe the gas flow from a shale gas well. The derivation of the flow equations and in particular the discretization scheme is based on the report *Modelling and Simulation of Shale Gas Reservoirs* by Knudsen (2010). The reader is referred to this report, or generally to Aziz and Settari (1979) for further details on the reservoir modeling.

2.1 Reservoir model

The physical process of the gas flow in shale gas reservoirs is complicated. Simplifications and approximations are necessary to describe the flow in the complex network of fractures, and comprehensive numerical simulations are normally required to describe these flow patterns. The applicability of these type of models to model-based optimization is thus limited. Analytical models of the gas flow in fractured reservoirs are normally obtained by dual-porosity mathematical models. These models have been extended to describe the gas production in tight gas and shale gas reservoirs. See for instance Medeiros et al. (2007) and Carlson and Mercer (1991) for examples on dual porosity models.

In this thesis, a model of the gas flow in a shale gas reservoir is constructed using a black oil based approach. The use of black-oil based models in shale gas reservoir modeling is limited, but the technique is well established and document from conventional reservoir modeling, making the modeling considerably easier. The essential idea is to use a *radial composite reservoir model* with two concentric region, each having homogeneous properties. To describe the highly conductive fractures in the stimulated region close to the

wellbore, the inner region is imposed a high permeability and a small radius, while the outer region retains the low permeability of the shale gas reservoir. Further assumptions of the reservoir model are:

- The flow is single phase.
- The geometry of the reservoir is cylindrical.
- The reservoir consist of only one layer.
- The entire thickness of the reservoir is perforated by a well in the center of the cylindrical reservoir model.

By using Darcy's law for laminar flow and assuming that the flow is one-dimensional and purely radial, the flow equation for the single phase gas flow in radial coordinates is described by the partial differential equation (PDE)

$$\frac{\partial}{\partial t}(\phi\rho) = \frac{1}{r}\frac{\partial}{\partial r}\left(r\rho\frac{k}{\mu}\frac{\partial p}{\partial r}\right) \tag{2.1}$$

where t is time, r the radial axis, ϕ the porosity, ρ density, k the permeability and μ the viscosity. The porosity is assumed constant, while the pressure dependency of the three parameters are omitted to simply the notations. Equation (2.1) assumes low flow velocity and thereby neglects the second order flow term often added to Darcy's law in the description of gas flow in a porous media. The gas density ρ is highly pressure dependent and is normally substituted with the real gas law

$$\rho = \frac{pM}{ZRT} \tag{2.2}$$

where M is molecular mass, Z the gas compressibility factor, R the universal gas constant and T the reservoir temperature. It is common to assume isothermal conditions in the reservoir, expressing the *total* compressibility c as

$$c = \frac{1}{\rho}\frac{\partial\rho}{\partial p}\bigg|_T \tag{2.3}$$

Gas expands with decreasing pressure and the disparity between gas rates measured in the reservoir and at the surface is therefore prominent. It has become conventional to express the gas flow rates standard conditions by the use of volume formation factors. For gas, the volume formation factor is defined (Aziz and Settari, 1979)

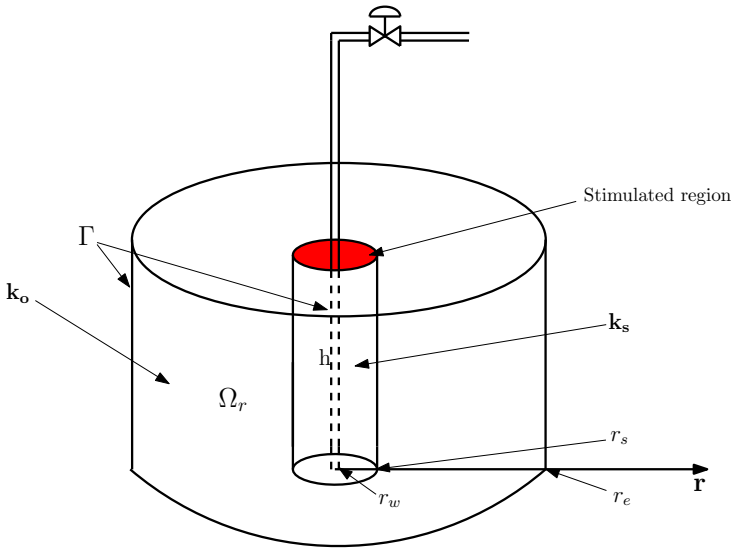

Figure 2.1: Illustration of reservoir geometry

$$B = \frac{TZp_{sc}}{T_{sc}p} \tag{2.4}$$

where p_{sc} and T_{sc} is the pressure and the temperature at standard conditions, 1 bar and 15.5°C, respectively.

The boundary conditions of the reservoir are defined with no flow across the outer boundary and a sink in the center of the reservoir. Equation (2.2) and (2.3) are substituted in the basic flow equation (2.1) with some rearrangements to obtain an applicable expression of the gas flow in reservoir, see Al-Hussainy et al. (1966). With respect to the reservoir geometry in figure 2.1, the general boundary value problem (BVP) for the gas flow in the reservoir is expressed

$$\phi \frac{p}{Z} c \frac{\partial p}{\partial t} = \frac{1}{r} \frac{\partial}{\partial r} \left(k \frac{p}{\mu Z} r \frac{\partial p}{\partial r} \right), \quad r_w < r < r_e \tag{2.5}$$

Boundary conditions

$$\left. \frac{\partial p}{\partial r} \right|_{r_e} = 0, \qquad \forall t > 0 \tag{2.6a}$$

$$\left. r \frac{\partial p}{\partial r} \right|_{r_w} = \frac{q_{sc} B \mu}{2\pi h k}, \qquad \forall t > 0 \tag{2.6b}$$

Initial conditions

$$p(r,0) = p_{\text{init}} \qquad \text{in} \quad \Omega_r \cup \Gamma \tag{2.7}$$

$$\Omega_r - \text{reservoir interior} \quad \Gamma - \text{reservoir boundary}$$

The boundary conditions (2.6) are *Neumann*-conditions as they describe the derivative of the pressure across the boundary. Equation (2.5) is a nonlinear PDE, but can be linearized in different ways depending on the range of pressure in the reservoir.

2.1.1 Linearization of the PDE

The viscosity μ and compressibility factor Z are both highly pressure dependent and the treatment of these parameters defines the appropriate linearization technique.

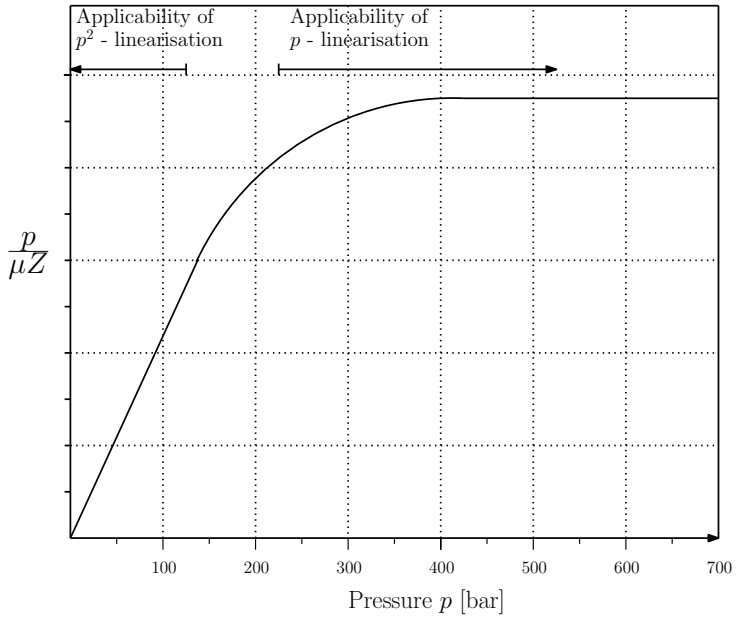

Figure 2.2: Illustration of the product $\frac{p}{\mu Z}$.

Consider the illustration in figure 2.2 of the fraction $p/\mu Z$, adapted from Golan and Whitson (1991) . A straight forward approach is to assume the fraction $p/\mu Z$ constant, which is a reasonable approximation for pressures higher than about 300 bar as indicated in the illustration in figure 2.2. For

pressures lower than about 200 bar, the product μZ can be assumed approximately constant. This approximation is known as the p^2-linearization, and is the as assuming small pressure gradients in the reservoir. Both these linearization techniques where studied in Knudsen (2010). In relation with a well-model, it is important to emphasize that both the reservoir pressure *and* the well bottomhole pressures must be within the specified pressure ranges for linearization techniques to be valid. It was observed that both these linearization-techniques limits the validity of the reservoir simulations.

To avoid limitations on the applicability of the reservoir model due to the pressure range in the reservoir and in the well, equation (2.5) will be expressed by the use of so-called pseudopressure, defined as (Al-Hussainy et al., 1966)

$$m(p) = 2\int_0^p \frac{p'}{\mu Z} dp' \tag{2.8}$$

The transformation (2.8) between pressure and pseudopressure $m(p)$ is nonlinear, but omits any assumptions about the gas compressibility factor Z and the viscosity μ. The left hand side of equation (2.5) can be rewritten

$$\phi\mu c \frac{p}{\mu Z}\frac{\partial p}{\partial t}$$

For notational convenience, the pressure argument of pseudopressure $m(p)$ is omitted in the rest of the report. The time derivative in terms of pseudopressure m can be expressed

$$\frac{\partial m}{\partial t} = \frac{\partial m}{\partial p}\frac{\partial p}{\partial t} = 2\frac{p}{\mu Z}\frac{\partial p}{\partial t}$$

and the spatial derivative is obtain in a similar way:

$$r\frac{\partial m}{\partial r} = r\frac{\partial m}{\partial p}\frac{\partial p}{\partial r} = 2\,r\frac{p}{\mu Z}\frac{\partial p}{\partial r}$$

Substituting these identities in the PDE in equation (2.5), the linearized PDE in terms of pseudopressure m yields

$$\boxed{\phi\mu c\frac{\partial m}{\partial t} = \frac{1}{r}\frac{\partial}{\partial r}\left(kr\frac{\partial m}{\partial r}\right)} \tag{2.9}$$

Equation (2.9) is linear in m when the coefficients are fixed and has the same form as the more well-known diffusivity equation. However, by the use of a radial composite reservoir model to describe the difference in permeability in the stimulated region from the shale, equation (2.9) becomes a nonlinear

PDE. In fact, both μ and the total compressibility c are highly pressure dependent. Generally speaking, the PDE in equation (2.9) is thus a nonlinear form of the diffusivity equation.

Boundary conditions and initial conditions are both adaptable to the flow equation in terms of pseudopressure m. Since

$$\left.\frac{\partial p}{\partial r}\right|_{r_e} = 0 \quad \Rightarrow \quad \left.\frac{\partial m}{\partial r}\right|_{r_e} = \left.\left(\frac{\partial m}{\partial p}\frac{\partial p}{\partial r}\right)\right|_{r_e} = 0 \tag{2.10}$$

The boundary condition on the inner boundary r_w, equation (2.6b) can be reformulated using the volume formation factor in (2.4):

$$r\left.\frac{\partial m}{\partial r}\right|_{r_w} = r\frac{\partial m}{\partial p}\left.\frac{\partial p}{\partial r}\right|_{r_w} = \frac{\partial m}{\partial p}\frac{q_{sc}B\mu}{2\pi hk} \tag{2.11}$$

$$= q_{sc}\frac{\partial m}{\partial p}\frac{\mu}{2\pi hk}\frac{TZp_{sc}}{T_{sc}p} \tag{2.12}$$

Since

$$\frac{\partial m}{\partial p} = 2\frac{p}{\mu Z}$$

the final form of the inner boundary can be expressed

$$r\left.\frac{\partial m}{\partial r}\right|_{r_w} = q_{sc}\frac{2p}{\mu Z}\frac{\mu}{2\pi hk}\frac{TZp_{sc}}{T_{sc}p} = q_{sc}\frac{Tp_{sc}}{T_{sc}\pi hk} \tag{2.13}$$

Formulating the initial pseudopressure m_{init} from the initial condition (2.7) is straight forward using the definition of the pseudopressure.

Mathematically, the use of a radial composite reservoir permeability can be expressed

$$k(r) = \begin{cases} k_s & r \leq r_s \\ k_o & r > r_s \end{cases} \tag{2.14}$$

As a result of the composite permeability, the PDE in equation (2.9) cannot be solved analytically. The reservoir model will therefore be evaluated numerically, using a spatial discretization of the pseudopressure m similar to conventional spatial discretization of single phase petroleum reservoirs.

In the rest of the report, it will be assumed that all flow rates are expressed in standard conditions. Hence the subscript sc, denoting standard conditions, is omitted in the notation of the gas flow rate q.

2.2 State space formulation

This section is heavily based on the work in Knudsen (2010), except for a different state variable due to the pseudopressure linearization. The main equations are repeated to present the numerical reservoir model. The applied discretization scheme of the reservoir model is the same as for single phase fluid.

The PDE describing the gas flow in the shale gas reservoir will be discretized using a finite difference scheme to approximate the spatial derivative. Dividing the reservoir into N_m grid blocks and defining the pseudopressure m_i as the block variable for grid block i, the state variables is stacked in a state vector

$$\mathbf{m} := \begin{bmatrix} m_1 & m_2 & \dots & m_{N_m} \end{bmatrix}^T \tag{2.15}$$

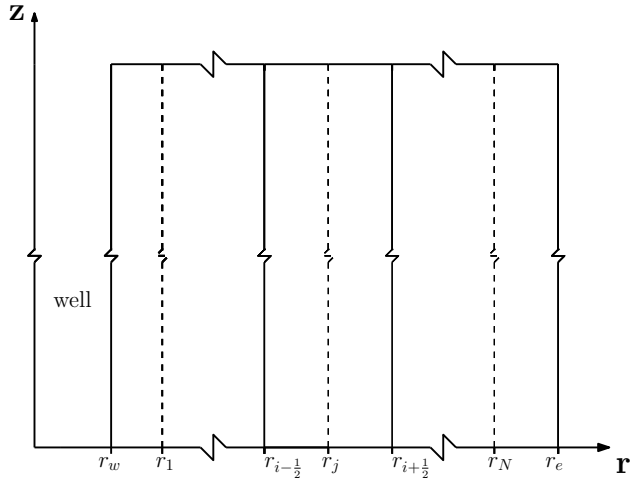

Figure 2.3: Grid definition. From Knudsen (2010)

The pseudopressure m_i for grid block i is obtained by applying the finite difference method on the PDE in equation (2.9)

$$\begin{aligned} &\pi \left(r_{i+\frac{1}{2}}^2 - r_{i-\frac{1}{2}}^2 \right) h \, \phi \mu c \frac{\partial m_i}{\partial t} = \\ &\quad 2\pi h \left[r_{i+\frac{1}{2}}^L k_{i+\frac{1}{2}} \left(\frac{m_{i+1} - m_i}{r_{i+1} - r_i} \right) - r_{i-\frac{1}{2}}^L k_{i-\frac{1}{2}} \left(\frac{m_i - m_{i-1}}{r_i - r_{i-1}} \right) \right] \end{aligned} \tag{2.16}$$

The boundary conditions in terms of m are incorporated in the numerical reservoir model by directly substituting equation (2.10) and (2.13) in the finite difference scheme for grid block N_m and grid block one, respectively. The grid block radii are defined such that

$$\ln \frac{r_{j+1}}{r_j} = constant \tag{2.17}$$

with a particular evaluation of $r_{i\pm\frac{1}{2}}$, $r^L_{i\pm\frac{1}{2}}$ and $k_{i\pm\frac{1}{2}}$. The derivation and details of these expressions, including a more thorough derivation of equation (2.16) and the boundaries are left out, and can be found in Knudsen (2010) or in textbooks on reservoir modeling as Aziz and Settari (1979) and Abou-Kassem et al. (2006).

The discretization of the PDE results in a set of ODE's, which in turn can be rearranged in a state space model. See for instance Chen (1999) for description of state space models. The spatial discretization of the boundary value problem for the flow in the shale gas reservoir can then be replaced by the single ordinary differential equation (ODE)

$$\mathbf{E}\dot{\mathbf{m}}(t) = \mathbf{A}\mathbf{m}(t) + \mathbf{B}q(t) \tag{2.18}$$

$$\mathbf{m}(0) = \mathbf{m_{init}} \tag{2.19}$$

where $q(t)$ corresponds to a scalar input since there is only a single well. The spatial discretization of the reservoir model is then with basis in equation (2.16) re-arranged in the matrices $\mathbf{A}$, $\mathbf{B}$ and $\mathbf{E}$:

$$\mathbf{A} := \begin{bmatrix} -a_{1+\frac{1}{2}} & a_{1+\frac{1}{2}} & 0 & \cdots & 0 \\ a_{2-\frac{1}{2}} & -\left(a_{2-\frac{1}{2}} + a_{2+\frac{1}{2}}\right) & a_{2+\frac{1}{2}} & \cdots & 0 \\ 0 & \ddots & \ddots & & 0 \\ 0 & 0 & \ddots & \ddots & 0 \\ 0 & \cdots & a_{N_m-1-\frac{1}{2}} & -\left(a_{N_m-1+\frac{1}{2}} + a_{N_m-1-\frac{1}{2}}\right) & a_{N_m-1+\frac{1}{2}} \\ 0 & 0 & \cdots & a_{N_m-\frac{1}{2}} & -a_{N_m-\frac{1}{2}} \end{bmatrix}$$

$$a_{i+\frac{1}{2}} := \frac{2\pi r^L_{i+\frac{1}{2}}\, k_{i+\frac{1}{2}}\, h}{r_{i+1} - r_i}, \qquad i = 1 \cdots N_m - 1$$

$$a_{i-\frac{1}{2}} := \frac{2\pi r^L_{i-\frac{1}{2}}\, k_{i-\frac{1}{2}}\, h}{r_i - r_{i-1}}, \qquad i = 2 \cdots N_m$$

$$\mathbf{E} := \begin{bmatrix} V_1\phi\mu c & 0 & \dots & 0 \\ 0 & V_2\phi\mu c & \dots & 0 \\ \vdots & 0 & \cdots & 0 \\ 0 & \dots & 0 & V_{N_m}\phi\mu c \end{bmatrix} \tag{2.20}$$

$$V_i = \pi \left(r_{i+\frac{1}{2}}^2 - r_{i-\frac{1}{2}}^2 \right) h \tag{2.21}$$

Observe that the compressibility c and the viscosity μ in matrix $\mathbf{E}$ are evaluated as constant values to obtain a time independent, constant matrix. The consequence of this assumption is discussed closer in section 3.3. Matrix $\mathbf{B}$ is derived from the discretization of grid block N_m, and is obtained

$$\mathbf{B} := \begin{bmatrix} -\frac{2Tp_{sc}}{T_{sc}} \\ 0 \\ \vdots \\ \vdots \\ 0 \end{bmatrix} \tag{2.22}$$

The matrices $\mathbf{A}, \mathbf{B}$ and $\mathbf{E}$ are all constant and independent of m if the coefficients are fixed. Note that the sum of the elements in each row of matrix $\mathbf{A}$ is zero. Hence $\mathbf{A}$ is singular.

2.3 Well representation

The gas inflow $q(t)$ from the reservoir in the well is often represented through a *well model* as a function of the bottomhole pressure p_{wf}, a valve setting α and the pressure in the grid block closest to the wellbore. For applicability to the reservoir model in derived in the previous section, the well model is represented in terms of the pseudopresure m. The well model is obtained from Darcy's flow law by including the volume formation factor to express the gas flow in surface rates. Using a skin factor S for correction of the ideal flow characteristics, the well model in terms of the pseudopressure m can be represented

$$q(t) = \alpha\, w\, [m_1(t) - m(p_{wf})] \tag{2.23}$$

$$w := \frac{\pi k h T_{sc}}{T p_{sc} \left(\ln \frac{r_1}{r_w} + S \right)} \tag{2.24}$$

where α is the valve setting, simply a fraction between 0 and 1. Note that the flow rate in both equation (2.23) as well as the rest of the report is represented in surface conditions. The term w in equation (2.24) is often referred to as the well index. It takes a particular simple form, due to the cylindrical reservoir geometry and the assumption of single phase flow.

Representing the well flow rate in terms of the bottomhole (pseudo)pressure and the valve setting, impacts the state space model of the pseudopressure in the reservoir. The final state space formulation depends on the definition of the control variable. If the valve setting α is absent and the bottomhole pressure p_{wf} is controlled directly, the well index w is subtracted from entry (1,1) in matrix $\mathbf{A}$ due to the minus sign in $\mathbf{B}$. The control variable u is then replaced by $m(p_{wf})$, and the resulting state space model will be nonlinear since μ and Z are uncontrollable and must be included in the nonlinear mapping from pressure to pseudopressure.

If the valve setting α can be controlled directly, matrix $\mathbf{B}$ be will be a function of the state vector, while matrix $\mathbf{A}$ remains a pressure independent matrix. Defining $\alpha(t)$ as the control variable, $u(t) := \alpha(t)$, the resulting state space formulation will be on the form

$$\mathbf{E}\dot{\mathbf{m}}(t) = \mathbf{A}\mathbf{m}(t) + \tilde{\mathbf{B}}\left(\mathbf{m}\left(t\right), m_{wf}\right)\alpha(t) \tag{2.25}$$

$$\mathbf{m}(0) = \mathbf{m_{init}} \tag{2.26}$$

where the notation m_{wf} is used as an abbreviation for the bottomhole pseudopressure. Equation (2.25) is a *bilinear* state space model (Verdult and Verhaegen, 2000), since it is linear in $\mathbf{m}$ if either α or $\mathbf{m}$ is fixed. Element $(1,1)$ in matrix B in equation (2.22) is replaced by

$$\tilde{\mathbf{B}}(1,1) = -\frac{2\pi kh}{\ln\frac{r_1}{r_w} + S}\left(m_1(t) - m_{wf}\right) \tag{2.27}$$

All other entries in $\mathbf{B}$ are still zero. The matrix $\mathbf{E}$ is invertible provided that the gas is compressible, i.e. $c \neq 0$. By left-multiplying equation (2.25) with $\mathbf{E^{-1}}$, the state space model can be expressed on "standard" form

$$\dot{\mathbf{m}}(t) = \bar{\mathbf{A}}\mathbf{m}(t) + \bar{\mathbf{B}}(\mathbf{m(t)}, m_{wf})\alpha(t) \tag{2.28}$$

$$\mathbf{m}(0) = \mathbf{m_{init}} \tag{2.29}$$

where $\bar{\mathbf{A}} = \mathbf{E^{-1}A}$, $\bar{\mathbf{B}} = \mathbf{E^{-1}}\tilde{\mathbf{B}}$. The three-diagonal pattern of matrix $\mathbf{A}$, common for the finite difference matrix of the PDE discretization in one spatial variable, is preserved using the valve setting as control variable.

2.4 Tubing performance

The pressure drop in the tubing is caused by gravity effects and friction between the gas and the tubing wall. Using the mechanical energy balance for a true vertical well, the pressure drop between the bottomhole of the well and the wellhead is expressed (Katz and Lee, 1990)

$$\int_{p_{wf}}^{p_w} v dp + m_g g z_w + m_g \frac{f z_w v^2}{2D_t} = 0 \tag{2.30}$$

where p_w is the wellhead pressure, v is the gas molar volume,f is the friction factor corresponding to the fully turbulent region of the Moody diagram, $z_w$is the true vertical depth of the well, D_t the tubing diameter and m_g the mass of the gas. By substituting equation (2.30) with real gas laws and evaluating the temperature and the compressibility factor Z at average values, the energy balance can be solved for steady state flow,

$$p_{wf}^2 = C_1 p_w^2 + C_2 q^2 \tag{2.31}$$

where C_1 and C_2 are constants. The common scheme for solving the gas deliverability of the reservoir is to use so-called *nodal analysis*, typically with a fixed wellhead pressure. See for instance Guo et al. (2007) or Golan and Whitson (1991). However, since the reservoir model is expressed in pseudopressure, this requires the solution of a set of nonlinear equations consisting of the flow from the reservoir and equation (2.31) for the tubing. This complicates the reservoir simulation and modeling considerably. Hence, the friction term in the tubing is neglected. Equation (2.30) is then solved with the surface as datum, linking the bottomhole pressure p_{wf} to the wellhead pressure p_w with the static relation (Knudsen, 2010)

$$p_{wf} = e^s p_w \tag{2.32}$$

$$s := \frac{z_w G M_{air}}{R T_a Z_a} \tag{2.33}$$

where $G = M/M_{air}$ is gas specific gravity and M_{air} is the molecular mass of air. The static ratio between the wellhead and the bottomhole pressure is then directly substituted in the well flow model in equation 2.23,

$$q(t) = \alpha\, w\, [m_1(t) - m(e^s p_w)] \tag{2.34}$$

Consequently, controlling the pressure or the valve setting at the bottomhole of the well is the same as controlling the same variables with respect to the

wellhead valve (choke). This, as there is no dynamics between the two pressures. Therefore, the it will be assumed that all control settings are posed on the *wellhead* valve.

The dynamics of the well flow and the pressure during the start up of a gas well or after a shut-in are complex and hard to model. These dynamics are not included in the mechanical energy balance in equation (2.30), but are governed by the Navier-Stokes equations. By using Darcy's law in the reservoir model, hence assuming stationary flow, the start-up dynamics of the well are lost. The result of these unmodeled dynamics is an unrealistic high flow rate immediately after the well is re-opened. Consequently, an upper bound on the flow rate is imposed:

$$q(t) \leq q_{max} \tag{2.35}$$

The upper bound on the flow rate thus limits the amount of gas extracted from the reservoir to physically realistic values. Hence, the upper bound also affect the pressure drop in the reservoir.

2.5 Numerical calculation of pseudopressures

All parameters in the integrand of the pseudopressure in equation (2.8), i.e. the viscosity and the compressibility factor in addition to the pressure itself, are pressure dependent functions. It is therefore necessary to know the PVT values of the gas evaluated at various pressures values to be able to evaluate the pseudopressures of the gas. The values used in this application is obtained by assuming knowledge of the reservoir temperature T and the gas gravity G. Calculation of the pseudopressures are done numerically by trapezoidal integration of the table values of p, μ and Z. Hence, each value of the pressure corresponds to one value of the pseudopressure.

The mapping of from pressure p to pseudopressure $m(p)$ is nonlinear. Figure 2.4 shows the correlation between pressure and pseudopressure, based on the the table values in appendix A.

For high pressure values, the function may be approximated by a linear function. To include the entire pressure range, the fitting of a polynomial function would be better, or possibly using a piecewise function. However, curve fitting of the pseudopressure function in figure 2.4 is omitted in this report. Instead, linear interpolation is used to obtain values of pressures and

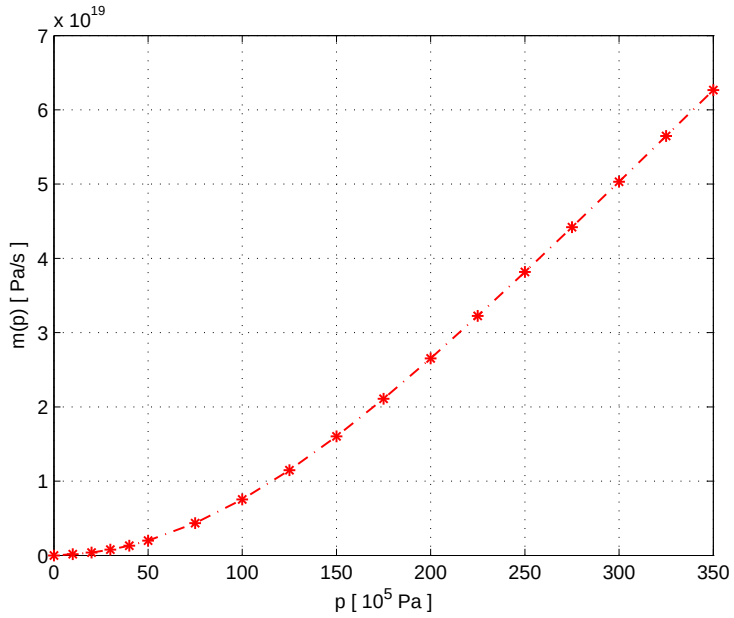

Figure 2.4: The nonlinear map from pressure p to pseudopressure $m(p)$. Observe the scale on the axes.

pseudopressures that are between the PVT table values in appendix A.

Chapter 3

The performance of shale gas wells

This chapter presents simulations and analysis of the performance of a single shale gas well based on the cylindrical reservoir model developed in chapter 2. Further, the problem of liquid loading in shale gas wells is addressed in this chapter. To review to the potential of applying shut-ins, a case study with constant shut-in times is presented at the end of the chapter.

3.1 Base case for the reservoir model

This section presents the reservoir geometry and a base case for reservoir properties used in the simulations in this chapter and also in the succeeding optimization in the next chapters.

The reservoir geometry will hold the same values for each of the wells considered in this report. The grid is constructed so that 8 grid block radii are

Table 3.1: Reservoir geometry

Parameter	SI-units	Field units
r_w	0.11 m	0.36 ft
r_e	914.4 m	3000 ft
h	152.4 m	500 ft
z_w	2300 m	10000 ft

inside the stimulated fractured region, stretching out to $r_s = 32\,\text{m}$. This is done to emphasize the pressure behavior inside the stimulated region, as

these pressures are considered to be more important for the flow compared to the pressure behavior close to the outer boundary of the reservoir. The gas flow in the developed shale gas reservoir is most sensitive to the magnitude of the reservoir permeability (Knudsen, 2010), which is also the parameter that is most difficult to determine in practice. Hence, variations in reservoir properties for different wells will consist of different rock permeability. The sensitivity of the permeability in the inner stimulated region was investigated in Knudsen (2010), and shown not to be decisive on the cumulative production. Values for the reservoir properties are given in table 3.2. Typical initial pressure in the Barnett Shale is in Cipolla et al. (2009) reported to be 3000 psia, which is about 207 bar.

Table 3.2: Reference reservoir properties

Parameter	SI-units	Field units
N_m	12	-
k_s	100 mD*	-
k_o	0.00075 mD	-
ϕ	5 %	-
S	0	-
r_s	32 m	105 ft
μ	$2.02 \cdot 10^{-5}$ Pa · s	$2.02 \cdot 10^{-3}$ cp
c	$8.46 \cdot 10^{-8}$ Pa^{-1}	$5.83 \cdot 10^{-4}$ psi^{-1}
T	366.3 K	200.0° F
$\mathbf{p_{init}}$	200 bar	2900 psi

* The SI-unit for permeability is m^2. However, for convenience, the established field unit for permeability mD is used. A - sign means that the field unit equals the SI-unit.

The average temperature T_a in the well is calculated as the arithmetic mean between the wellhead temperature and the reservoir temperature, while the average gas compressibility factor Z_a corresponds to arithmetic mean between Z evaluated at wellhead pressure and initial reservoir pressure. Table 3.3 summarizes the tubing, the wellhead and the gas properties.

Table 3.3: Tubing and surface conditions

Parameter	SI-units	Field units
p_{sc}	1 bar	14.5 psi
T_{sc}	288.15 K	59.3°F
D_t	6 cm	2.4 in
M_{air}	0.029 kg/mol	-
R	8.31 J/Kmol	-
T_w	311 K	100.4°F
G	0.7	-

3.2 Production profile of shale gas wells

Shale gas wells share many of the same production characteristics, of which the rapid decline of productivity is the most dominating. This is supported by the report "World Energy Outlook 2009" from the International Energy Agency - IEA (WEO, 2009), which provides a detailed study of the potential, the last decade's production history and current production level of shale gas. In particular, the report gives the summary of a study of more than 7000 Barnett shale wells. The production profiles were observed to be remarkably similar, both for horizontal and vertical wells. To elaborate, the wells exhibited an early peak in the production before a rapid decline in the rate. For horizontal Barnett wells, the decline in production rate is reported to be averagely 39% during the first year and 50% from the first to the third year. Vertical wells appears to have a slightly slower decline in rate. The monthly rates are reported to decline as much as 57% over the first 12 months.

The averagely initial monthly production rate for Barnett shale horizontal wells, is in the report from IEA showed to be approximately 0.9 million m^3. Based on this value, the maximum daily flow rate q_{max} for the base case is set to 30000 m^3/d. Using the reservoir geometry and parameter values in the base in tables 3.1 - 3.3, a simulation of the production from a shale gas well over a time horizon of 5 years is shown in figure 3.1(a). The the wellhead pressure is set to a constant value of 10 bar.

The reservoir model model is implemented in the Simulink toolbox in MATLAB, and the simulations are executed with the variable step solver `ODE15s` in Simulink. The solver is based on a backward differential integration scheme (BDF) and is suitable for integration of numerically stiff systems ODE's.

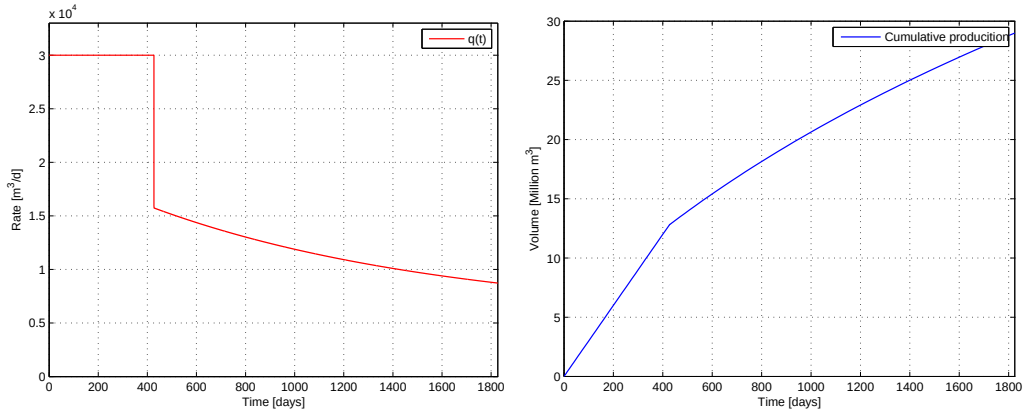

(a) Flow rate (b) Cumulative production

Figure 3.1: Typical production profile of a single shale gas well

Without enforcing the maximum production rate, the initial peak in production rate would in the magnitude of 10^9, obviously unrealistic high. By imposing the maximum rate constraint of 30000 m^3/d, the shale gas reservoir is enable of provide enough pressure to maintain this production level for approximately 400 days. The decline in production rate is then steep. By zooming in on the point of the sudden drop in the rate, it can be seen that the transition time from 30000 m^3/d to about 15700 m^3/d is less than 12 hours. In reality, this transition will last longer, start earlier and be smoother. The reason for the abrupt fall in the rate comes from both simplifications and assumptions in the modelling as well as the numerical integration. The steep decline in the production rate also illustrates the numerical issues associated with the integration of the numerically stiff the state-space model describing the shale gas reservoir, particularly in the transition from the initial plateau level to the fast dynamics present when the rate drops. It should also be noted that the derivative of $q(t)$ in the region of the abrupt production drop is close to infinity, or at least very high. This may cause problems when the model is applied in model-based optimization. A long slowly decreasing production rate is achieved in the last years of the simulation.

Figure 3.1(b) shows the profile of the cumulative production. The total cumulative production increases linearly the first 400 days when the well is producing at the constant maximum rate, and the total production over five years is about 29 million m^3. As comparison, in the study of the ultimate recovery of the Barnett shale wells in WEO (2009), the mean recovery of a Barnett shale horizontal well was found to be 38.6 million m^3. The ultimate recovery of vertical wells is significantly lower; the mean is 20.7 mcm. How-

ever, it is important to remark that figure 3.1(b) as well as figure 3.1(b) is not physically realistic: in reality, the probability of liquid accumulation in the well is high, which will cause erratic flow rates or eventually kill the well if not appropriately treated. Hence the curve of the cumulative production will in realty fluctuate substantially more than in figure 3.1(b).

The grid pressures for the same example are shown in figure 3.2. Comparing the behavior of the grid pressures with the flow characteristic in figure 3.1(a), the thick "multicolored" line shows that the pressures inside the stimulated region drops with approximately the same factor until the pressure reaches the constant bottomhole pressure $p_{wf} = e^s p_w$. The difference in pressure drop is most prominent the first days after the opening of the well, while this difference is offset due to the imposed maximum rate q_{max}. At this point, the flow drops from its plateau level while the grid pressures in the stimulated region stays just above p_{wf}. The gas flow in the well is now dominated by the amount of gas flowing from the low permeable outer region of the reservoir to the high permeable stimulated region.

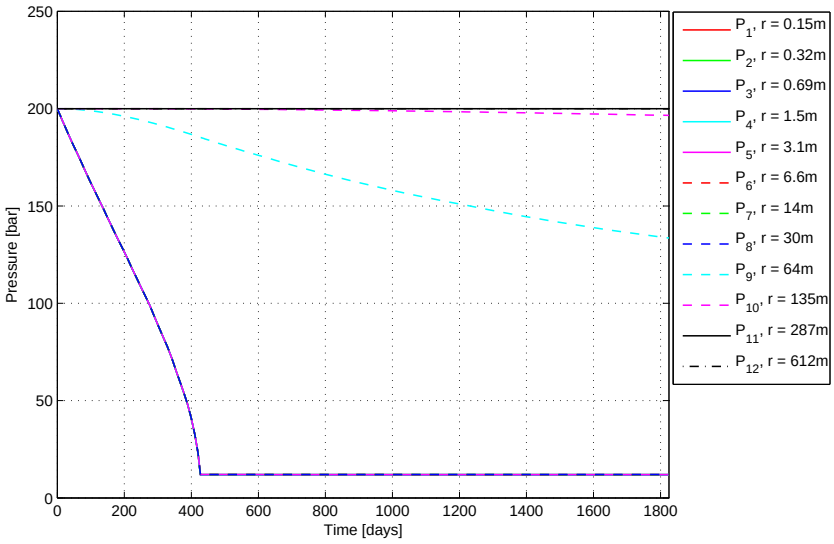

Figure 3.2: Grid pressures

Although the wellhead pressure is included as a constant value in the simulations, it must be regulated to keep a constant plateau level in the initial phase if the *actual* peek production is higher. However, it is important to remark that the plateau level caused by the upper bound on the flow rate is a compensation for the lack of dynamics in the tubing model. In reality, this

plateau level may not exist and the flow rate will then naturally decline.

Before proceeding on the shale gas well performance, a model validation and comparison is performed against a commercial reservoir simulator.

3.3 Model validation

As mentioned in the derivation of the reservoir model, an analytical solution of the PDE is not available due to the radial composite permeability. A commercial reservoir simulator is therefore used to compare and validate the numerical model of the reservoir. The reservoir model with the geometrical properties of table 3.1 and the reservoir parameter values as in table 3.2 has been implemented in the compositional and black oil reservoir simulator SENSOR from Coats Engineering, Inc[1]. The typical shale gas flow characteristic in figure 3.1(a) is compared with a corresponding SENSOR model in figure 3.3. The initial reservoir pressure and the maximum production rate are the same as in the base case in section 3.2, 200 bar and 30000 m^3/d respectively. It is remarked that the interval of values of p, μ and Z used to calculate the pseudopressures for the MATLAB model is significantly shorter than for the values in the black-oil PVT table used in the SENSOR model.

The errors in the MATLAB model are most prominent in the transition region from the initial plateau in the rate to the slowly decreasing rate. This is a result of the assumption of constant compressibility and initial viscosity in the PDE (2.9) and equivalently in matrix $\mathbf{E}$ in the state space formulation. The compressibility increases with lower pressure, and gives smoother transient behavior as seen in the graph for the SENSOR model. Although the assumption ensures an numerically efficient model with constant matrices, it limits the achievable accuracy of the model. An improvement of the MATLAB model would be to either use interpolation of the table values of c and μ (see appendix A) or to use the first order correction of the total compressibility,

$$c = \frac{1}{p}$$

where the (second-order) effect of the gas compressibility factor Z on the total compressibility c is neglected. Both corrections would improve the accuracy of the model and the resemblance between the output from SENSOR model and the MATLAB model. However, this would result in a numerically more

[1] http://www.coatsengineering.com/

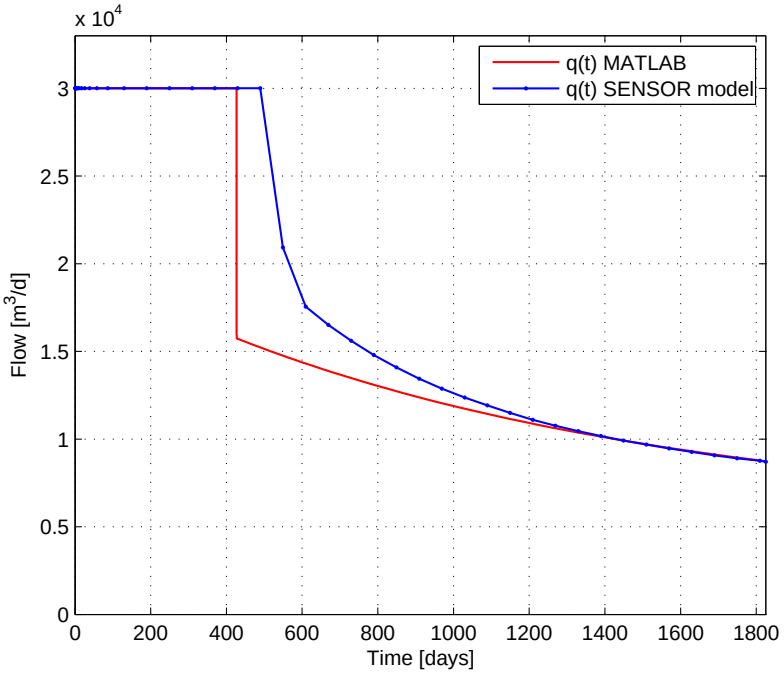

Figure 3.3: Comparison of MATLAB and SENSOR reservoir model.

demanding reservoir model. Some of the loss of accuracy of the MATLAB model is also due to the simple tubing model without friction compensation. By convention, the product of c and μ are normally evaluated at initial pressure or as the arithmetic mean between the well pressure and the initial reservoir pressure. In this application, μ is evaluated at initial conditions while c is chosen as a physically consist value, corresponding to evaluation at a pressure between the constant wellhead pressure and the initial reservoir pressure.

The total error in cumulative production between the to models over the five years prediction time is 6.35%.

3.3.1 Applicability to horizontal wells

Historically, most of the drilling in shale gas reservoirs has consisted of vertical wells (Jenkins and Boyer II, 2008). With the improvements in drilling technology in the mid-1990s, horizontal wells became and attractive and economically profitable alternative. Today, the use of horizontal and multilateral wells has become the preferred drilling technology, and more than 90% of all new wells in the Barnett shale are being developed with horizontal

wells (Jenkins and Boyer II, 2008).

The driving force for the gas flow in shale gas reservoirs is the pressure gradient between the wellbore and the reservoir. Gravity effects on the gas are small compared to the pressure gradients, and can thus be neglected in the flow equation without substantial loss of model accuracy. The use of a vertical well model with cylindrical geometry will therefore not loose essential applicability to horizontal wells. The use of a cylindrical coordinates, imposing radial flow in the reservoir is also generally advantageous in the description of the fractures compared in the stimulated region compared to the use of Cartesian coordinates. However, what actually is vital and decisive for the productivity of horizontal as well as vertical wells, is the number of stages of hydraulic fracturing. Essentially, each stage of the hydraulic fracturing will cause a thin layer of high conductivity lateral of the well. Compared to the single layer reservoir model used in this report, the production will only be boosted in this thin layer and not along the complete well. This will clearly decrease the gas rate, and somewhat change the flow pattern. However, the development of a multi-layered horizontal shale gas well is left out for further work.

3.4 Liquid loading

Shale gas wells are prone to liquid loading. As the gas in shale is normally only semi-dry, *condensate* will be entrained in the extracted gas. The condensate may cause liquid accumulation in the well and hence increase the backpressure on the vertical parts of the well significantly. As the pressure in the near wellbore part of the reservoir decreases, the back pressure on the well will eventually become to high for the liquid to be "lifted" out of the well. This phenomenon is known as liquid loading, and will cause erratic production before the well eventually will die.

Turner et al. (1969) proposed an estimate of the critical gas velocity needed to ensure continuous removal of liquids. This rate is also known as the "minimum rate to lift". The estimate is widely used, and is expressed

$$v_{gc} = 6.2 \frac{\left[\sigma \left(\rho_l - \rho\right)\right]^{0.25}}{\rho^{0.5}} \tag{3.1}$$

where the constant in front is converted to SI-units (20.4 in original paper). Note that ρ is here implicitly interpreted as the *gas* density. The real gas

law in equation (2.2) can be used to substitute ρ, expressing the molecular weight of the gas M as a function of specific gas gravity G:

$$\rho = \frac{GM_{air}}{ZRT} p \tag{3.2}$$

It was suggested in Turner et al. (1969) that the onset of liquid load-up is dominated by the wellhead conditions. The temperature and the compressibility factor Z generally varies with the pressure in the well, and are easiest evaluated at values corresponding to the wellhead pressure. Numerical values for the liquid density ρ_l and the interfacial tension σ must be specified. Using the suggested values from Turner et al. (1969), these are set to

- $\sigma = 0.06\,\mathrm{N/m^2}$
- $\rho_l = 1074\,\mathrm{kg/m^3}$

Denoting the tubing cross section areal A_t and , the critical gas rate in $\mathrm{m^3/d}$ expressed in standard conditions are

$$\begin{aligned} q_{gc} &= 8.64 \cdot 10^4 A_t \frac{p_w\, T_{sc}}{p_{sc} T_w Z_w}\, v_{gc}(p_w) \\ v_{gc}(p_w) &= 6.2 \frac{\left[\sigma\left(\rho_l - \kappa\, p_w\right)\right]^{0.25}}{\kappa\, p_w^{0.5}} \\ \kappa &:= \frac{GM_{air}}{Z_w R T_w} \end{aligned} \tag{3.3}$$

The size of the cross section of the tubing will obviously affect the necessary rate for continuous removal of liquids in the well. From the critical rate (3.3), small tubing diameters are thus an advantage for avoiding liquid loading in the well.

The original Turner constant 6.2 has been observed to be conservative and not necessarily reliable as many gas wells produce at rate less than the critical gas rate (Petroleum Experts Ltd., 2008). In the same Prosper reference manual from the Petroleum Experts Ltd, it is also suggested that the value might be changed by the user depending on the application. Li et al. (2001) proposed the value 2.5 for the constant after analyzing and observing the typical shape of a liquid drop entrained in gas streams. The values were tested against field data and showed convincing results when compared to the actual production rate.

In Al-Ahmadi et al. (2010), field data of the flow rates from a random chosen Barnett shale gas wells have been compared to the critical rate given by Turner et al. (1969). The flow rates that fell below the theoretical critical rate, were in most of the collected field data observed as erratic and unstable flow rates. The liquid loading was started after about 300 days, and were persistent after 400 days. In shale gas wells, onset of liquid loading may generally occur earlier than expected due to the stimulation with hydraulics, leaving undrained water in the fractures.

The different literature presented above on liquid loading in gas wells and in particular the determination of the critical gas rate q_{gc}, indicates some freedom in the choice of the constant in front of the critical gas rate equation (3.1). Choosing a value close to the original Turner constant will ensure a reasonable margin on the critical rate. Choosing the constant 5.0 and using a wellhead pressure of 10 bar together with the gas properties given in table 3.3 leads to the critical rate $q_{gc} = 1.203 \cdot 10^4\,\mathrm{m}^3/\mathrm{d}$. This value will be imposed as the minimum accepted gas rate in the following optimization, applied with a means of preventing liquid loading in the well.

The calculated value of the critical rate is applied in a simulation in the next section, using a cyclic production strategy for the shale gas reservoir model.

3.5 Cyclic production with predefined shut-in time

To review the potential of using a shut-in based production optimization, this section studies the use of a simple *cyclic* production strategy of a single shale gas well, based on the above discussion on liquid accumulation the well. This as a first review of the shut-in based production strategy.
Applying a cyclic production pattern to shale gas wells without accounting for the possibility of liquid loading in the well is generally unfavorable. This may cause sudden shut-ins of the well and thus deviation in the original production plan. The interpretation of the critical rate needed to ensure continuous removal of accumulated liquid in the well is therefore emphasized in the development of the production strategy. To study the effect on the total gas production from shut-ins triggered by the minimum rate, a set of simulations is performed using a constant shut-in time t_{SI} for each of the simulations, but with a different shut-in time for each the simulations. The specifications are:

- The reservoir properties are the same as in the simulation of the reservoir model in section 3.1 with initial reservoir pressure 200 bar and constant 10 bar wellhead pressure. The prediction time is five years.

- The maximum flow rate is set to $3 \cdot 10^4\,\mathrm{m}^3/\mathrm{d}$, and the minimum rate is set equal to the critical rate, $q_{gc} = 1.203 \cdot 10^4\,\mathrm{m}^3/\mathrm{d}$.

- Once the well rate falls below minimum rate, the well is shut-in for the fixed predefined time t_{SI}. After t_{SI} shut-in-days, the well is re-opened and set to produce again, provided that the rate does not violate the minimum rate. When the rate once again falls below q_{gc}, the well is shut-in for another t_{SI} days.

- The considered shut-in times are from one to 100 days. Figure 3.4 is attached to illustrate the flow rate with 100 days equivalent shut-in days. The shut-in time is exaggerated to illustrate the shut-in pattern.

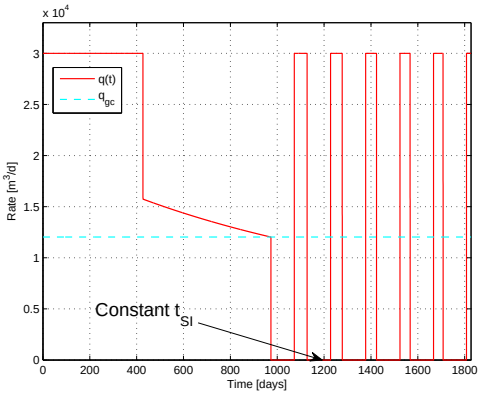

Figure 3.4: The production rate with constant 100 days shut-in time

The simulations are done using the reservoir model implemented in Simulink in MATLAB, and the shut-ins are implemented with logical constraints and measurements of the rate. Hence there is no optimization involved in the obtained results, only simulations.

Figure 3.5 shows the total cumulative production over five years as a function of the predefined (constant) shut-in time t_{SI}. The total cumulative production decreases slowly as a function of the shut-in time. Based on the linear least-squares fit, the cumulative production decreases with

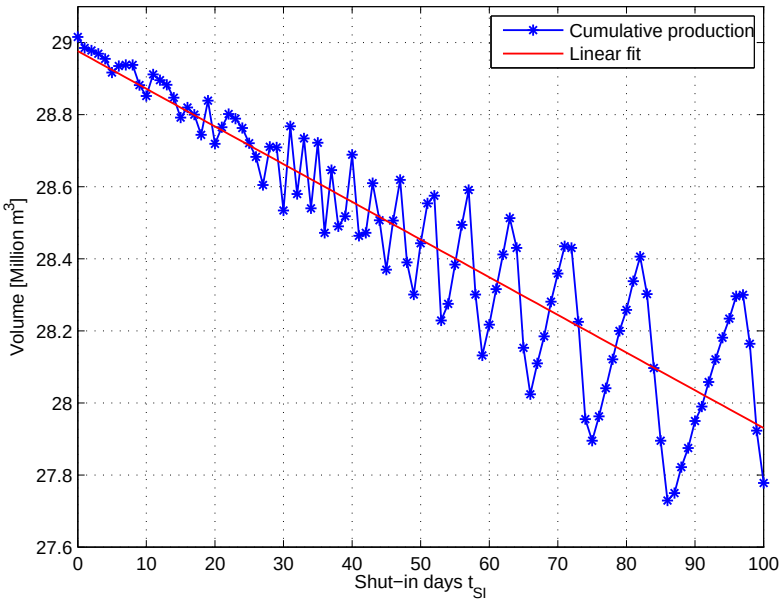

Figure 3.5: Cumulative production as a function of a fixed number of shut-in days t_{SI} for each shut-in. The prediction time is 5 years.

$$q_{cum.}(t, t_{SI}) \approx 28.98 - 0.0105\, t_{SI} \quad [10^6 \text{ m}^3]$$

as a function of the equivalent shut-in time. However, the total cumulative production only decreases with 4.26% by using a shut-in time of 100 days. To elaborate, using a 100 days equivalent shut-in period each time the well falls below the critical rate, the well is shut-in 6 times during 5 years. Hence the well is shut almost 33% of the prediction time, still being able of extract more than 95% of the maximum possible recovery if *no* liquid loading occur.

However, there is *no* particular reason why the optimal production strategy is to use an equivalent shut-in time each time the well must be shut-in. It may be beneficial to initially apply short shut-ins, while longer shut-ins may be beneficial when the well has been operated for several years. The switching frequency and shut-in times may also be affected by varying gas prices, discounting of the sales-income, cost involved in the production and constraints in the switching capacity. These factors and the above discussion are used as basis in the next chapter when the optimization problem for maximizing the asset of shale gas wells is formulated.

Chapter 4

Optimization of gas production

This chapter presents the derivation of the optimization problems with the objective to maximize the production from one and multiple shale gas wells. Two different optimization problems is defined, with different operational settings and constraints.

The essential idea of the optimization is to apply shut-ins with variable duration. This will cause the gas to flow from the outer low-permeable region of the reservoir to the inner high-permeable region, does recharging the fractures in the stimulated region with gas. This, as a means of preventing liquid loading and boosting the production. The derivation of the optimization problems is based on the simulations and analysis on the production profile of shale gas wells in chapter 3.

4.1 System description

The production optimization of shale gas wells considered in this report consist of the production from a given number of wells with a joint production planning. Both optimization from a single well production and from multiple wells is considered. The optimization problem is therefore defined to be applicable with respect to both of these cases. In order to maintain a relatively high production rate over the wells life-cycle, the wellhead pressure must be kept low for shale gas wells. The wellhead pressure will normally not be able to provide high enough pressures for the gas to flow in pipelines from the production fields to the market. Hence, a compressor is needed to compress the gas to a certain higher pressure. However, the integration of the compressor in the modeling is limited with the means of keeping the complexity level low, thus focusing on the *shut-ins* of the wells in problem formulation.

Figure 4.1 illustrates the production facilities. The need for separation of the gas is normally limited, and a separation unit is therefore left out in the system description.

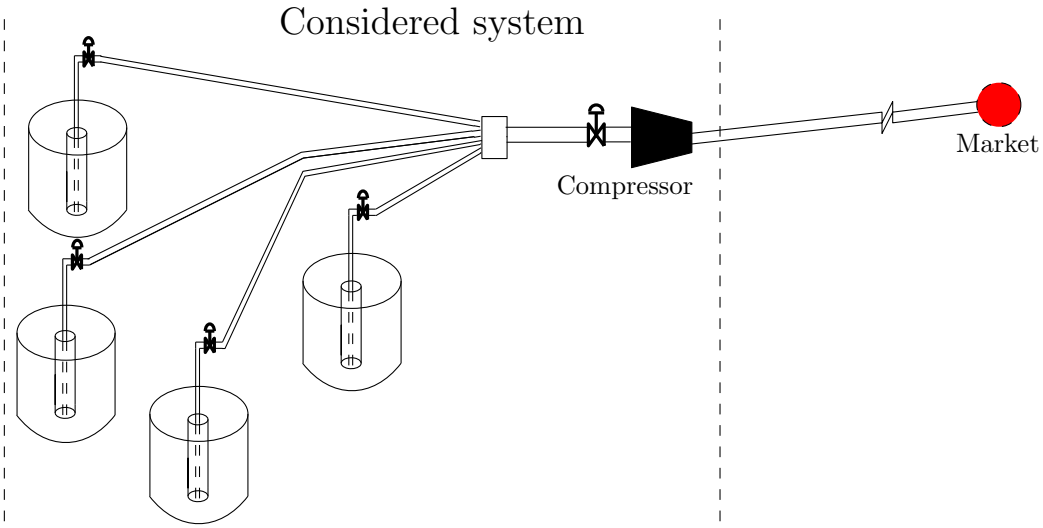

Figure 4.1: Illustration of production facilities for shale gas wells

4.2 Objective function

In the choice of objective when optimizing the production from oil and gas reservoirs, it it common to maximize either the cumulative production or the net present value (NPV). If the objective is to maximize the NPV, there is a choice in whether to include only the revenue from the sold gas or also including the cost of producing the gas. Further, if the latter expenditures are integrated in the objective function, there is a freedom in whether only operational expenditures (OPEX) or also capital expenditures (CAPEX) is included. The CAPEX of shale gas wells dominated by the drilling costs and the cost of stimulation with hydraulic fracturing. The OPEX of a set of shale gas wells consists of on-site costs of operating the wells and preparing the gas to be sold to the market. These costs are associated with the gas compression, manpower costs, transportation costs and tear and wear of the well and surface equipment. The definition of the objective function will therefore take different forms depending on the level of integration of economics. The choice of objective functions therefore consists of:

1. Maximizing the cumulative production without taking economy into account

2. Maximizing the NPV including operational expenses (OPEX) and/or capital expenditure (CAPEX).

Table 4.1: Sets and indices

Index	Meaning	Set	Meaning
i	grid block number	N_m	number of grid blocks
j	well number	r	set of wells
k	time step	N	number of time steps

The objective function in the definition of the optimization problems is chosen to be option two with the OPEX as the only included expenditures. That is, the objective is to optimize the NPV with respect to the operation costs of the wells. The use of NPV as optimization criteria includes a discount factor d_f representing the today value of money, defined as a yearly interest rate. The objective function will be evaluated over a time horizon T. Letting G_p denote the gas price in US dollars ($) per volume-unit, the objective of maximizing the NPV can be written :

$$\max \int_0^T \left\{ G_p \sum_{j=1}^{r} q^j(t) - C_{op}(t) \right\} \frac{1}{(1+d_f)^t} dt \tag{4.1}$$

By considering short-term production, the objective function (4.1) can be interpreted as the *operating income* by imposing a zero discount factor d_f. The term $C_{op}(t)$ is used to represent the on-site costs of operating the wells and preparing the gas to be sold to the market.

As mentioned, the largest expenditure of shale gas wells is without cost of the drilling and the hydraulic fracturing. The stimulation may performed on a regular basis, depending on the geological properties of the rock and the success of each stimulation, and thus be very expensive. In fact, this is one of the reasons why many shale gas wells today still are unprofitable (WEO, 2009). However, these costs are difficult to estimate, and there is not much literature available on the topic. These costs are therefore not included in the objective function (4.1). Hence, the NPV optimized over a long time horizon will not include all of the expenditures related shale gas wells, but only include operational costs, excluding any stimulation with hydraulic fracturing

performed after the initial completion of the well.

4.2.1 The cost term

The production costs of shale gas wells are among other related to the cost of compressing the the gas. The cost term in the objective function will therefore include a crude estimate of the cost of compressing the gas.

In calculations of the power needed to compress the gas, it will be assumed that the compressor is a so-called *reciprocating* compressor. Further, a constant downstream pressure p_m will be assumed. This pressure is decided by the demands and requirements of the market. It is common to assume an isotropic process for reciprocating compression of gases (Guo et al., 2007). Letting p_c be the compressor inlet pressure and neglecting the kinetic energy in the expression of the shaft work, the power consumption for the compressor can be written (Guo et al., 2007)

$$w_s(t) = \frac{k_g}{k_g - 1} p_c \, q(t) \left[\left(\frac{p_m}{p_c} \right)^{\frac{k_g - 1}{k_g}} - 1 \right] \tag{4.2}$$

where $q_(t)$ is the gas to be compressed and k_g is the gas specific heat ratio[1]. Normally, several stages of compression is required to compress the gas up to the specified pressure p_m. This will modify the power expression slightly.

The fuel consumption of the compressor is a function of the power capacity and the power used, the load on the prime mover and type of fuel used. The function is normally given by the compressor specifications or obtained by estimation. This cost will not be included in the costs of the compressor. The power cost is therefore imposed as the only compression cost. Implicitly, it is thus assumed that the compressor runs on the power supply and that all gas that is produced can be sold to the market. For more details on multiple stage gas compression, fuel consumption and appurtenant power expressions, see Guo et al. (2007).

Using P_p to represent the power price in US dollars ($) per kWh, the cost term is written

[1]The subscript g is used to separated the gas specific heat ratio, normally denoted $k = \frac{c_p}{c_v}$, from the time step index k.

$$C_{op}(t) = l(q(t), t) + P_p w_s(t) \tag{4.3}$$

The time argument of l are used to impose a variable cost on operation of the wells. This term is aimed on operation costs and switching costs of the well, and will be addressed below.

4.2.2 The time horizon

The time horizon of scheduling and production planning of oil and gas wells may be subdivided into long-term, mid-term and short-term planning. Long-term planning often concerns strategic management and investments related to operating the set of wells and equipment involved in the gas production. The time horizon is typically a year and up to the field's lifetime. Mid-term planning typically spans the production planning and reservoir management in the time scale of months up to a couple of years, and is also referred to as season planning in the literature. Short-term production planning is more related to operational production planning. The operator will typically seek to optimize the daily production based on the up to date production history of the well and available real-time information. The time horizon is thus typically days or weeks. Short term production planning of petroleum systems has recently been gained a lot of interest, and is usually denoted real-time production optimization (RTPO). See for instance Gunnerud and Foss (2009) for an application example of RTPO and Bieker et al. (2006) for an extensive overview of the aspects of RTPO.

The problems considered is this report consider production optimization of shale gas wells on short term and long term horizons. The study of long term optimization is used to study long terms effects and production potential over several years, while the short term production optimization is aimed for the daily scheduling, the production planning and the need for maintenance of the wells.

4.3 Reservoir model representation

The chosen strategy to represent the reservoir and well model in the optimization problem, is to use a so called *simultaneous* approach. In this way, the reservoir and well model model is directly integrated in the optimization problem. That is, the optimization and simulation are performed simultaneously. The opposite is to use a *sequential* approach, where each iteration in the optimization algorithm consist of the system

model simulation and the optimization performed sequentially. The pros and cons of both approaches is addressed in chapter 7, while for now it is remarked that the simultaneous approach results in many optimization variables and constraints while preserving full control of the reservoir model equations with respect to the optimization.

4.3.1 Time discretization

The state space model (4.7) is discretized in time to be incorporated in the optimization algorithm. An implicit integration method is desirable when the time integration is solved using a fixed step size. The simplest and least accurate implicit integration method is implicit Euler's method. Compared to the well-known explicit Euler's method, the integration is done *backwards* in time. In terms of a general ODE,

$$\dot{\mathbf{m}} = f(\mathbf{m}, \mathbf{u})$$

the right-hand side is expanded

$$\frac{\mathbf{m}_{k+1} - \mathbf{m}_k}{h} = f(\mathbf{m_{k+1}}, \mathbf{u_{k+1}}) \tag{4.4}$$

The number of time steps is defined $N = T/h$, where h is the fixed step size and T is the prediction time. The state space model of the gas reservoir and the well model are kept as separate equality constraints in the implementation. This as a means of discussing different control variables with respect to the optimization problems, but also as the well model will be extended to include the imposed maximum flow rate q_{max}. With respect to the state space model in equation (2.18), (2.19) and well model in equation (2.34), the discrete representation is obtained by using (4.4),

$$\frac{\mathbf{m}_{k+1} - \mathbf{m}_k}{h} = \mathbf{E^{-1}A}\mathbf{m}_{k+1} + \mathbf{E^{-1}B}q_{k+1} \tag{4.5}$$

$$\underbrace{\left(\mathbf{I} - \mathbf{E^{-1}A}h\right)}_{=\mathbf{A_d}} \mathbf{m}_{k+1} = \mathbf{m}_k + \underbrace{\mathbf{E^{-1}B}h}_{=\mathbf{B_d}} q_{k+1} \tag{4.6}$$

The representation of r wells in the simultaneous optimization approach is then obtained by the equations

$$\mathbf{A_d}^j \, \mathbf{m}^j_{k+1} = \mathbf{m}^j_k + \mathbf{B_d}^j q^j_{k+1}, \qquad k = 0, .., N\text{–}1, \; j = 1, .., r \tag{4.7}$$

$$\mathbf{m}^j_0 = \mathbf{m}^j_{\mathbf{init}}, \qquad j = 1, .., r \tag{4.8}$$

$$q^j_k = \alpha^j_k \, w^j \left(m^j_{1,k} - m(e^s p^j_{w,k})\right), \qquad k = 0, .., N, \; j = 1, .., r \tag{4.9}$$

For each time step, the pseudopressure for each block together the separate well model are implemented as a set of explicit equality constraints. Hence, for *one* well the number of equality constraints representing the gas rate over the prediction time T is $(N_m + 1) \times (N + 1)$. Implicit Euler's discretization scheme is A-stable, that is, it is stable for any choice of the time step h (Egeland and Gravdahl, 2003) .

Before proceeding on the choice of control variables, the imposed bounds on the flow rate is discussed.

4.4 Bounds on the flow rate

As discussed in the modeling of the tubing performance in section 2.4, the production immediately following the re-opening of a well will be unrealistic high if no upper bound is posed on the flow rate q. This results in a quick depletion of the reservoir. To obtain realistic solutions from the production optimization, it will therefore be essential to impose a distinct upper bound on the flow rate from each well:

$$q_k^j \leq q_{max}^j, \qquad k = 0, .., N,\ j = 1, .., r \tag{4.10}$$

To prevent liquid loading in the wells, each of the flow rates should be greater than the critical gas rate specified q_{gc} derived in section 3.4. This rate is emphasized in the optimization and imposed as a *fixed* minimum rate for each well:

$$q_{gc}^j \leq q_k^j, \qquad k = 0, .., N,\ j = 1, .., r \tag{4.11}$$

Hence, the total bounds on q_k^j will be

$$q_{gc}^j \leq q_k^j \leq q_{max}^j, \qquad k = 0, .., N,\ j = 1, .., r \tag{4.12}$$

The lower bound in (4.12) will cause infeasibility once a well is shut in. To circumvent this problem, one possibility would be to soften the lower bound by introducing slack variable and penalize the slack variable in the objective function. However, penalizing the slack variable in the objective function will deteriorate the economical interpretation of the objective function. Hence this solution procedure will not be further investigated.

Equation (4.11) must be modified before implemented in the optimization problem. Its final form depends on the choice of decision variables.

4.5 Choice of control variables

Choosing the control variables of the wells for incorporation in the optimization formulation, consists of the options:

- Choosing which of variables in the well model in equation (4.9) to be control variables
- If the valve setting is chosen as control variable, it can be defined either as continuous or as integer variable.

The use of integer variables is an intuitive and straight forward approach for the modeling of shut-ins. Using integer variables to model on/off valves is also meaningful modeling approach. The pressure build-up in the reservoir from shut-ins of the well, is triggered by the valve setting α being set to zero, giving a step response in the grid pressures. This is property is essential, both for the simulation and for the optimization of the switchings of a shale gas well. There is no obvious way of implementing shut-ins by only controlling the wellhead pressure and at the same time avoiding integer variables, without assuming a particular structure of the optimal solution. Using integer variables enables an efficient way of handling the lower bound on the flow rate in equation (4.11). It is, however, important to mention that the solution procedure and implementation changes considerably once integer variables are introduced in the problem formulation.

The valve settings are by definition fractions between zero and one. Following the above discussion, the valve setting will therefore be imposed as integer *binary* variables. Following the notation of Wolsey (1998) for n-dimensional 0,1 vectors, the set of feasible valve settings will thus be a subsets of

$$\mathcal{B} = \{0\,,1\}^n$$

Although the frequency of the decision variables may be defined differently from the sampling interval of the state space model, it will be assumed that the control settings can be changed by the same interval as the fixed step size of the discretized reservoir model in equation (4.7). That is, the number of control variables will be the same as the number of time steps N.

The upper bound on the flow rates, q_{max}, complicates the problem formulation by the use of binary valve settings. If the wellhead pressure is fixed and the binary valve settings are chosen as the only control variables, the upper bound in equation (4.10) will cause an infeasible optimization

formulation. Actually, the only feasible production setting will be to shut the wells the entire prediction horizon. This infeasibility problem can be overcome by

1. Imposing the wellhead pressure for each time step as an additional control variable, thus introducing a a new decision variable in the optimization problem. The control variables will then be both the wellhead pressures and the binary valve settings.

2. Including the fixed maximum flow rate q^j_{max} in a reformulation of the well flow model in equation (4.9), using only the binary valve settings as control variables.

3. The same as above, but imposing a slack on the maximum flow rate. That is, the requested flow rate is included as a decision variable with tight bounds.

Option 2 is the strategy giving the least number of *control variables*, and is the preferred approach with the objective of modeling on/off valves. The intention of the optimization is to provide production plans and scheduling by the use of *shut-ins* of the wells. Hence, few control variables is advantageous.

The following optimization problems will therefore be defined with binary valve settings as the only control variables in a extended well model.

4.6 Mixed integer formulations

Based on the above discussion of objectives, constraints, bounds and decision variables, the optimization problem for one and multiple wells are formulated. The optimization will be performed using the discretized representation of the reservoir model in section 4.3.1. The objective function will thus be on the form,

$$\max \quad \sum_{k=0}^{N-1} \sum_{j=1}^{r} \frac{G_p q_k^j - C_{op,k}}{(1+d_f)^a} \, h \tag{4.13}$$

where a substitutes the time argument in the continuous time objective function (4.1), and yields the number of year passed since the start in the production.

4.6.1 Problem 1:

When the wellhead pressure is fixed, the upper bound (4.10) on the flow from the well model (4.9) will as mentioned cause infeasibility in the optimization problem. This problem is solved by replacing the upper bound q^j_{max} and the well model for each well j by the non-smooth, continuous function

$$q^j_k := \min\left\{q^j_{max}\,,\, \alpha^j_k\, w^j\left(m^j_{1,k} - m(e^s p^j_w)\right)\right\}, k = 0,..,N,\ j = 1,..,r \quad (4.14)$$

The lower bound (4.11) defining the shut-in rate can then be efficiently reformulated by the constraint

$$q^j_{gc}\alpha^j_k \leq q^j_k, \qquad k = 0,..,N,\ j = 1,..,r \quad (4.15)$$

thereby avoiding the infeasibility on (4.12) rising from shut-ins of a well. Note that this formulation is only meaningful when the valve settings are defined as binary variables. It is further remarked that the derivative of (4.14) is discontinuous and therefore may cause convergence problems in gradient based optimization algorithms. However, the need for additional *control* variables is avoided.

To enable the use of a variable cost on the *switchings* of the wells instead of the daily operation costs, the auxiliary variables η^j_k is introduce to count the number of switchings of a well. The η^j_k variables are defined by using the valve settings α^j_k in the additional constraints

$$|\alpha^j_{k+1} - \alpha^j_k| \leq \eta^j_{k+1}, \qquad k = 0,..,N\text{–}1,\ j = 1,..,r \quad (4.16)$$

A cost on the switchings of the wells can the be imposed in the general cost-term l in the objective function by

$$l(q^j_k) := O_p\, \eta^j_k, \quad (4.17)$$

where O_p is the price for opening or closing of a well in association with shut-ins. Since the sign in front of $C_{op,k}$ in the objective function is negative, symbolizing a *cost*, η^j_k will take the following values for time step $k+1$:

Event	α_{k+1}^j	α_k^j	η_{k+1}^j
closing	0	1	1
stay closed	0	0	0
opening	1	0	1
stay open	1	1	0

Note that that η variables are a defined as continuous variables, but only takes the values zero or one. The initial switching of the well can be defined by using the last valve settings prior to the prediction horizon, α_{-1}^j, defined such that

$$\alpha_{-1}^j = \begin{cases} 0, & \text{if the well is initially closed} \\ 1, & \text{if the well is initially open} \end{cases} \tag{4.18}$$

Including the constraint (4.16) and a price on η_k^j in the objective function will thus impose a cost on the switching of a well in addition to the cost of compressing the gas. These are the only operational costs included in the optimization formulation. When applying shut-ins as production plan of the shale gas wells, the operator will normally not have unlimited capacity to switch a large number of wells on and off. Hence there might be constraints on the acceptable number of switchings. This is incorporated as *global production constraints* on the switching of the wells, and imposed as a set of linear constraints on η_k^j, written generally as:

$$\Psi\left(\eta_1^1, \eta_2^1, ..., \eta_k^j, ..., \eta_N^r\right) = 0 \tag{4.19}$$

The constraints on the switching may be imposed both as per-time-step constraints and as constraints over the entire prediction horizon.

Summarized, the optimization problem in terms of maximizing the net present value for a set of shale gas wells controlled with on/off valve settings is formulated:

Problem 1:

$$\max \quad J = \sum_{k=0}^{N-1} \sum_{j=1}^{r} \frac{G_p\, q_k^j - C_{op,k}^j}{(1+d_f)^a}\, h \tag{4.20}$$

s.t.

$$\begin{aligned}
\alpha_k^j &\in \{0\,,1\}\,, && k=0,..,N,\ j=1,..,r \\
{\mathbf{A_d}}^j\ \mathbf{m}_{k+1}^j &= \mathbf{m}_k^j + {\mathbf{B_d}}^j q_{k+1}^j, && k=0,..,N\text{–}1,\ j=1,..,r \\
\mathbf{m}_0^j &= \mathbf{m}_{\mathbf{init}}^j, && j=1,..,r \\
q_k^j &= \min\left\{q_{max}^j\,, \alpha_k^j\, w^j\left(m_{1,k}^j - m(e^s p_w^j)\right)\right\}, && k=0,..,N,\ j=1,..,r \\
q_{gc}^j \alpha_k^j &\le q_k^j, && k=0,..,N,\ j=1,..,r \\
|\alpha_{k+1}^j - \alpha_k^j| &\le \eta_{k+1}^j, && k=0,..,N\text{–}1,\ j=1,..,r \\
\Psi\left(\eta_1^1, \eta_2^1, ..., \eta_k^j, ..., \eta_N^r\right) &= 0, \\
C_{op,k}^j &= O_p \eta_k^j + P_p\, \frac{k_g}{k_g-1} p_c\, q_k^j \left[\left(\frac{p_m}{p_c}\right)^{\frac{k_g-1}{k_g}} - 1\right]
\end{aligned}$$

By defining the valve setting as binary variables, problem 1 will consequently be a mixed integer nonlinear program (MINLP). Although problem 1 is formulated as the problem of finding the optimal set of binary valve settings, the entire set of optimization variables includes both continuous and integer variables. The cost term in the last line in the problem formulation is implemented in the objective function is written as a separate equation to simplify the readability.

Note that there are *no* pressure dependency or interconnections between the wellhead pressures of the different wells nor the inlet pressure of the compressor. It is assumed that all wells operates with a constant wellhead pressure, and the surface condition that the wells "see" is therefore the constant wellhead pressure p_w^j. With reference to figure 4.1 of the system description, it is thus assumed that there are additional valves in the inlet to the compressor inlet pressure. However, it is chosen not to include neither the description of these valves or the dynamics of the compression. The compression cost in the last line in the problem formulation will therefore only affect the *value* of the NPV as an estimate of the compression cost. Since it linearly adds up the compression cost from the individual flow rates, the argument of the optimal solution will not be affected by the compression cost term. This

way the integration of the surface and the subsurface system is done using a "loose coupling" scheme, with interconnections only in the *global production constraints*. The same level of integration is utilized in the definition of problem 2 below.

4.6.2 Problem 2:

Problem 2 is based on the following production scenario:

Based on the market's demands for natural gas, the customer of the gas produced from the considered shale gas wells has specified a requested supply of gas. From this request of gas, a supervisory control has specified a constant total production rate per time step for the set of wells controlled. The total gas rate demanded by the marked, denoted $q_{tot,k}$, is then expressed in standard conditions before the compression of the gas. Consequently, the specification of a total gas rate per time step from the r wells is imposed as a *global constraint* in a optimization problem with the same reservoir and well model as in the previous problem definition.

This type of problem resemble the problem of optimal trajectory following, where in this case the optimal trajectory is the constant rate. The most commonly used objective for such problem is to minimize the deviation from the optimal trajectory using a quadratic criteria. By choosing appropriate penalty parameters in the objective function matrices, the quadratic criteria ensures a high cost when there is a large deviation from the actual and the requested rate (the trajectory).

The drawback of using a quadratic criteria, is the loss of the economical meaning of the objective function. As will be shown in chapter 5, the particular form of the well model makes it possible to reformulate the nonlinearities by linear constraints and binary variables. Hence, it is an advantage to preserve linearity of the objective function. An alternative formulation that preserves both linearity and the economical meaning of the objective function is

$$J = \sum_{k=0}^{N-1} \left[\sum_{j=1}^{r} \left(G_p \, q_k^j \right) - P_p \, w_{s,k} - G_1 q_{1,k} - G_2 q_{2,k} \right] h \tag{4.21}$$

with the constraints

$$-q_{1,k} + q_{2,k} + \sum_{j=1}^{r} q_k^j = q_{tot,k}\,, \qquad k = 0, .., N-1 \tag{4.22}$$

The auxiliary variables $q_{1,k}$ and $q_{2,k}$ thus balance the total produced rate for each time step, and gives the r wells *total* deviation in production rate form the requested total rate per time step $q_{tot,k}$. The penalty parameters G_1 and G_2 are the price in \$ per volume unit that is lost from either producing too much or too less gas compared to the requested rate, respectively. This allows for different penalties on excessive gas production and underproduction. In particular, they can be interpreted both as economical parameters as well as tuning parameters for minimal deviation from the requested rate.

The flow rate from each well is still lower bounded by the specified critical rate q_{gc}^j. The estimate of the cost of the gas compression is now included as the only operation cost.

The optimization problem of with respect to maximizing the profitability of the set of shale gas wells under a total maximum production constraints therefore takes the form:

Problem 2:

$$\max \quad J = \sum_{k=0}^{N-1} \left[\sum_{j=1}^{r} \left(G_p\, q_k^j \right) - P_p\, w_{s,k} - G_1 q_{1,k} - G_2 q_{2,k} \right] h \tag{4.23}$$

s.t.

$$\begin{aligned}
\alpha_k^j &\in \{0\,, 1\}\,, && k = 0, .., N,\ j = 1, .., r \\
q_{tot,k} &= \sum_{j=1}^{r} (q_k^j) - q_{1,k} + q_{2,k}, && k = 0, .., N\text{–}1 \\
\mathbf{A_d}^j\ \mathbf{m}_{k+1}^j &= \mathbf{m}_k^j + \mathbf{B_d}^j q_{k+1}^j, && k = 0, .., N\text{–}1,\ j = 1, .., r \\
\mathbf{m}_0^j &= \mathbf{m}_{\mathbf{init}}^j, && j = 1, .., r \\
q_k^j &= \min \left\{ q_{max}^j\,, \alpha_k^j\, w^j \left(m_{1,k}^j - m(e^s p_w^j) \right) \right\}, && k = 0, .., N,\ j = 1, .., r \\
q_{gc}^j \alpha_k^j &\leq q_k^j, && k = 0, .., N,\ j = 1, .., r \\
w_{s,k} &= P_p \frac{k_g}{k_g - 1} p_c \sum_{j=1}^{r} (q_k^j) \left[\left(\frac{p_m}{p_c} \right)^{\frac{k_g - 1}{k_g}} - 1 \right]
\end{aligned}$$

Note that the requested rate may very well be time-varying, giving a sequence of different rates to follow instead of the same rate for each time step. However, the rate per time step will be assumed to be constant in this report. Problem 2 will only be considered on a short time horizon, therefore neglecting any discount factor. As in problem 1, there is no pressure dependency between the wells nor the compressor, and the global production constraints on the wells are therefore the requested total production rate.

Chapter 5

Implementation and solution methods

The use of integer variables in the formulation of the optimization problems in section 4.6, requires the use of solvers tailored for solving mixed integer programming. Generally, the Optimization Toolbox in MATLAB is not designed for mixed integer programs, and the availability of suitable solvers is rather limited. To enable efficient use of special purpose software tailored for mixed integer programs, the optimization problems from chapter 4 is implemented in the high-level mathematical programming languages GAMS [1] and Xpress-Mosel[2].

Both optimization problems in the previous chapter are implemented using the *simultaneous* approach. By doing so, the reservoir and well model equations are formulated as explicit equality constraints. This limits the complexity in the implementations while at the same time resulting in a large set of constraints and variables.

This chapter presents a reformulation of the MINLP problems in chapter 4 to a MILP problem by using linear constraints and additional binary variables. Hence, GAMS is used in the implementation of the MINLP problems, while Xpress-Mosel is used to implement a MILP reformulation of the problems. In addition, the mathematics of the optimization algorithms are briefly reviewed. At the end of the chapter, two alternative problem formulations are presented and addressed.

[1] GAMS Development Corporation, see `http://gams.com/`
[2] FICO ™, see `www.fico.com`

5.1 Solving mixed integer nonlinear programs

With the MATLAB model of the shale gas reservoir as basis, the optimization problem 1 in section 4.6 is implemented in the programming language GAMS (General Algebraic Modeling System). There are a variety of solvers distributed with GAMS, some of which are open-source and thus easily available for large-scale optimization.

The chosen optimizer for solving the implemented MINLP problem is the special purpose solver BONMIN (Basic Open-Source Nonlinear Mixed Integer programming), distributed through the COIN-OR project (Computational Infrastructure for Operations Research). The mathematical details of the various algorithms implemented in BONMIN can be found in Bonami et al. (2008). Of the four available algorithms in BONMIN for solving MINLPs, the branch and bound is selected due to the nonconvexity of the problems considered. This agrees with the recommendations in Bonami and Lee (2007). BONMIN further uses the open-source interior-point filter line-search algorithm IPOPT for solving the nonlinear programs (NLP) at the nodes with the integer variables relaxed.

5.2 Reformulation of the nonlinearities

The nonlinearities in the optimization problem formulations in section 4.6 are due to the extended well model

$$q_k^j := \min\left\{q_{max}^j\,,\alpha_k^j\,w^j\left(m_{1,k}^j - m(e^s p_w^j)\right)\right\}, k = 0,..,N,\ j = 1,..,r \quad (5.1)$$

and the definition of the η_k^j variables in equation (4.16). The nonlinearities in (5.1) consist of the aggregate function (the minimum value) and the product of α_k^j and $m_{1,k}^j$. Both these nonlinearities can be efficiently reformulated to *linear* constraints in a single binary or continuous variable. This enables reformulation of the original problems to mixed integer linear programs (MILP). The reformulation can be performed in several ways, and is a topic of several textbooks on mathematical programming and operation research. See for instance Williams (1993). The reformulation used in this section is based on the Xpress-MP manual from FICO^{TM} (2009).

For simplicity, the well index in (5.1) is left out in the derivation of the reformulations. Hence, it is implicitly assumed that the equations in the reformulation are valid for all of the wells considered.

5.2.1 Product values

Consider once more the non-smooth, aggregate flow function (4.14) for a fixed wellhead pressure p_w:

$$q_k = \min\left\{q_{max}\,,\, \alpha_k\, w\,(m_{1,k} - m(e^s p_w))\right\} \tag{5.2}$$

Define the actual well model, that is, the last term in the above expression

$$\tilde{q}_k := \alpha_k\, w\,(m_{1,k} - m_{wf}) \tag{5.3}$$

where $m_{wf} = m(e^s p_w)$ is the bottomhole pseudopressure corresponding to the fixed wellhead pressure p_w. Note that the nonlinear mapping $p_w \mapsto m_{wf}$ is done off-line, prior to the optimization. For readability, $\tilde{q}$ is divided into a nonlinear and a linear part, respectively:

$$\begin{aligned} &\tilde{q}_k = \alpha_k\, w\, m_{1,k} \;-\; \alpha_k\, w\, m_{wf} = \tilde{q}_{nl,k} \;-\; \alpha_k\, w\, m_{wf} \\ &\Rightarrow \tilde{q}_{nl,k} := \alpha_k\, w\, m_{1,k} \end{aligned} \tag{5.4}$$

The nonlinear part $\tilde{q}_{nl}$, is a product of one binary variable and one continuous variable. For the reformulation, it is necessary to know the bounds on the continuous variable m_1. Since there is no injection wells in the reservoir, the pressure will never go above the initial pressure, or equivalently, m_1 is upper bounded by the initial pseudopressure in grid block one. For producing wells, the block pseudopressures in the reservoir will never fall below the bottomhole pseudopressure m_{wf}. The equivalent mixed linear reformulation of $\tilde{q}_{nl,k}$, can then be obtained

$$\begin{gathered} \tilde{q}_{nl,k} = \alpha_k\, w\, m_{1,k} \\ \Downarrow \\ \begin{gathered} \alpha_k\, w\, m_{wf} \;\le\; \tilde{q}_{nl,k} \;\le\; \alpha_k\, w\, m^{max} \\ w\, m_{wf}\,(1-\alpha_k) \;\le\; w\, m_{1,k} \;-\; \tilde{q}_{nl,k} \;\le\; w\, m^{max}\,(1-\alpha_k) \end{gathered} \end{gathered} \tag{5.5}$$

where the maximum value of $m_{1,k}$, denoted m^{max}, equals the initial pseudopressure in grid block one. The inequalities (5.5) above are all linear, and

can hence substitute the nonlinear terms $\tilde{q}_{nl,k}$ in equation (5.4) in a MILP implementation.

5.2.2 Minimum values

In a similar, the $\min\{\cdots\}$ function in (5.2) can be reformulated as a set of linear constraints for implementation with a MILP solver. Using equation (5.3) for $\tilde{q}$, still omitting the well index, the flow equation (4.14) is repeated here with the simplified notation

$$q_k = \min\{q_{max},\, \tilde{q}_k\} \tag{5.6}$$
$$\tilde{q}_k := \tilde{q}_{nl,k} - \alpha_k\, w\, m_{wf} \tag{5.7}$$
$$\tilde{q}_{nl,k} := \alpha_k\, w\, m_{1,k} \tag{5.8}$$

It is necessary to know the lower and the upper bounds on the variable arguments in (5.6), in this case the lower and upper bound of $\tilde{q}$. The upper bound for $\tilde{q}$ is essentially given by the supremum norm of a sequence of all feasible values of (5.7) in the prediction horizon. However, when the wellhead pressure is fixed, the value upper bound on $\tilde{q}$, denoted $\tilde{q_k}^{\infty}$ is given by

$$\tilde{q_k}^{\infty} = w\,(m^{max} - m(e^s p_w)) \tag{5.9}$$

where m^{max} is the maximum value of pseudopressure $m_{1,k}$ in grid block one. Note that the value of $\tilde{q_k}^{\infty}$ is generally different for the individual wells and depends on the initial reservoir pressure. The lower bound on $\tilde{q}_k$ In the linear reformulation of the $\min\{\cdots\}$ function, one new binary variables d_1 is introduced for each time step. The $\min\{\cdots\}$ function expressing the well flow rate in problem 1 and 2 can then be reformulated with following set of linear constraints:

$$q_k \;\leq\; q_{max} \tag{5.10}$$
$$q_k \;\leq\; \tilde{q}_k \tag{5.11}$$
$$q_k \;\geq\; q_{max}\, d_{1,k} \tag{5.12}$$
$$q_k \;\geq\; \tilde{q}_k - \tilde{q_k}^{\infty}\, d_{1,k} \tag{5.13}$$

Note that the calculation of $\tilde{q_k}^{\infty}$ is done off-line and the value is thus known a priori the optimization. Observe the difference between this value and the

value q_{max}.

The equation defining the switchings,

$$|\alpha_{k+1} - \alpha_k| \leq \eta_{k+1}$$

is reformulated simply using the definition of the absolute value:

$$-\eta_{k+1} \leq \alpha_{k+1} - \alpha_k \leq \eta_{k+1}$$

5.2.3 Mixed integer *linear* formulation

To summarize the above reformulations, the complete reformulation of the extended well model is given below:

$$q_k = \min\{q_{max}, \alpha_k w (m_{1,k} - m(e^s p_w))\}$$

$$\Downarrow$$

$$\begin{aligned}
\tilde{q}_{nl,k} &\geq \alpha_k w m_{wf} \\
\tilde{q}_{nl,k} &\leq \alpha_k w m^{max} \\
w m_{1,k} - \tilde{q}_{nl,k} &\geq w m_{wf}(1 - \alpha_k) \\
w m_{1,k} - \tilde{q}_{nl,k} &\leq w m^{max}(1 - \alpha_k) \\
\tilde{q}_k &= \tilde{q}_{nl,k} - \alpha_k w m_{wf} \\
q_k &\leq q_{max} \\
q_k &\leq \tilde{q}_k \\
q_k &\geq q_{max} d_{1,k} \\
q_k &\geq \tilde{q}_k - \tilde{q}_k^{\infty} d_{1,k}
\end{aligned} \tag{5.14}$$

All other constraints in addition to the objective function takes the same form as in the problem definitions in section 4.6. These are not restated here. The MINLP problems defined in problem 1 and 2 are now effectively reformulated as equivalent MILP problems. In fact, the optimization problem considered is by using the above reformulations recasted as *mixed binary linear programs* (MBP) or mixed 0-1 programs (Pochet and Wolsey (2006), chapter 3). However, the implementation with the reformulation of the nonlinearities will be referred to the as MILP formulation in the rest of the report.

It is clear that the reformulation of the product and the $\min\{\cdots\}$ function is not free of cost; for each time step k, the single nonlinear constraint (5.2)

of the well flow is replaced by nine inequality constraints and one additional binary variable for each well. In addition, the absolute value for counting the switchings is replaced by two linear constraints.

The MILP problems are implemented in the state of the art software Xpress-IVE from FICO^{TM}, using the special purpose mathematical programming language Xpress-Mosel. The MILP implementation in Xpress-IVE will be the implementation in focus in this report. The optimizer applied on the MILP problem is referred to as the Xpress-MP solver, and is briefly presented below.

Remark on the MILP implementation: Note the difference between imposed well-model (5.1) with the above reformulation with a reformulation of the form

$$\begin{aligned} q_k &\leq \alpha_k \, w \, (m_{1,k} - m(e^s p_w)) \\ q_{gc}\alpha_k &\leq q_k \leq q^j_{max} \end{aligned}$$

Although the above formulation would avoid the additional binary variables $d_{1,k}$, the result would be different since q_k is now defined as *free* variable with two (redundant) upper bounds. In the simultaneous implementation, this will cause a different result and flow behavior than the aggregate well flow function (5.1). It is hence important to emphasize that the $\min\{\cdots\}$ form of the extended well model (5.1) is imposed as a compensation for the simplicity of the tubing model, giving physically more realistic flow rates.

5.3 Optimality conditions

This section briefly reviews the main properties of the Branch and Bound algorithm. Although both the MINLP implementation in BONMIN and the MILP implementation is solved with basis in the Branch and Bound algorithm, the nonconvexity of the formulated MINLP problem causes a somewhat different structure of the solution and the search tree. This is further addressed in the discussion in section 7.3. Hence, the details below are related to the MILP formulation with the Xpress-MP optimizer. The section is based on Pochet and Wolsey (2006).

The Xpress-MP optimizer uses a *relaxation* of a subset of the binary variables solved as a linear program by using the Dual *Simplex* Method. The MILP

problem is the solved as a sequence of linear programs by using the Branch and Bound algorithm. To simplify the discussion of the algorithm, a general formulation of the variables and constraints defining the MILP problem is made. The complete feasible set X of variables and linear constraints defining the MILP pressed can be expressed (Pochet and Wolsey, 2006)

$$X = \{(x, \theta) \in \mathbb{R} \times \{0, 1\} \quad : \quad \Lambda\, x + \Omega\theta \geq \upsilon\} \tag{5.15}$$

where all continuous variables are lumped into one long vector x and the binary variables are lumped into the vector θ. The coefficients of the linear constraints can be re-arranged in the large matrices Λ and Ω, including the vector υ. The size of the sets are omitted and thus implicitly understood in the set definition. Initially, all binary variables are relaxed and the initial linear relaxation (LR) is solved at the root node. That is, the maximum of the objective value J is solved with respect to the relaxed set

$$P_x = \{(x, \theta) \in \mathbb{R} \times [0, 1] \quad : \quad \Lambda\, x + \Omega\theta \geq \upsilon\} \tag{5.16}$$

For a mixed binary *linear* program with a maximization objective function, the solution $\bar{J}$ of the initial LR defines an upper bound on the optimal objective value of the original MILP problem (Wolsey, 1998). That is,

$$J(X) \leq \bar{J}(P_x) \tag{5.17}$$

Due to linearity of all of the constraints from the MILP reformulation, the solution obtained from the Simplex solver of the LR problem is *globally* optimal. On the the other hand, the objective value $\underline{J}$ of any feasible solution with respect to the MILP problem provides a lower bound on the optimal objective value. Hence, the bounds on J are

$$\underline{J} \leq J(X) \leq \bar{J}(P_x) \tag{5.18}$$

These bounds are crucial in the optimization of an MILP problem. In the Xpress-MP optimizer, it is defined [3]

$$\text{Duality gap} = \frac{|\text{Best LB} - \text{Best UB}|}{\text{Best UB}} \times 100[\%] \tag{5.19}$$

The best lower bound LB is updated every time a better feasible solution is found, and is initially set to $\underline{J} = -\infty$. In a similar way, the initial best UB is $\bar{J}(P_x)$. At run time, the best UB is updated with the maximum upper bound among all outstanding nodes to be solved. The value is obtained from

[3]The definition differs form the definition in Pochet and Wolsey (2006) as it divides by the best upper bound instead of the best lower bound.

the subsequent LP relaxations, for which a subset of the binary variables are fixed and one variable is branched at a time. The set of fixed binary variables follows from the rules for the node selection and the variable branching. Both rules have important impact on the quality of the solution. See for instance Pochet and Wolsey (2006) for a discussion on different definitions of these rules.

The duality gap is very important property for solving MILP's with the branch and bound algorithm, and is applied in the termination of the search for the optimal solution. It will therefore be emphasized in the numerical tests of the MILP implementation in the next chapter.

5.4 Scaling

The magnitude of the pseudopressures may cause numerical related problems in the optimization. An initial reservoir pressure of $p = 200\,\text{bar}$ $(2.0 \cdot 10^7\,\text{Pa})$ corresponds to an initial pseudopressure $m(p) = 2.65 \cdot 10^{19}\,\text{Pa/s}$. The pseudopressure variables $\mathbf{m}$ should therefore be scaled before fed to the optimization solver. The scaling of $\mathbf{m}$ is performed using *diagonal scaling* (Nocedal and Wright, 1998), which allows different scaling of the individual grid block variables:

$$\mathbf{m} := \mathbf{M_s}\tilde{\mathbf{m}} \tag{5.20}$$

with diagonal scaling matrix

$$\mathbf{M_s} := \begin{bmatrix} m_{s1} & 0 & & \\ 0 & m_{s2} & \ddots & \\ & \ddots & \ddots & 0 \\ & & 0 & m_{sNr} \end{bmatrix} \tag{5.21}$$

The initial reservoir pseudopressure $\mathbf{m_{init}}$ is scaled as above, while m^{max} used in the reformulations in section 5.2 and the bottomhole pseudopressure m_{wf} are scaled with the factor m_{s1}. The vector $\mathbf{m}$ is thus replaced by the product $\mathbf{M_s}\tilde{\mathbf{m}}$ in state space equation for each well, giving

$$\mathbf{A_d}\mathbf{M_s}\ \tilde{\mathbf{m}}_{k+1} = \mathbf{M_s}\tilde{\mathbf{m}}_k + \mathbf{B_d}q_{k+1} \qquad k = 0 \cdots N-1 \tag{5.22}$$

The scaling matrix $\mathbf{M_s}$ is invertible if every individual diagonal entry is non-zero. Hence, left-multiplying equation (5.22) with $\mathbf{M_s}^{-1}$ gives the *scaled* state space model as a set of equality constraints:

$$\tilde{\mathbf{A}}_\mathbf{d}\ \tilde{\mathbf{m}}_{k+1} = \tilde{\mathbf{m}}_k + \tilde{\mathbf{B}}_\mathbf{d} q_{k+1} \qquad k = 0 \cdots N-1 \qquad (5.23)$$
$$\tilde{\mathbf{A}}_\mathbf{d} := {\mathbf{M_s}}^{-1}\mathbf{A_d}\mathbf{M_s}$$
$$\tilde{\mathbf{B}}_\mathbf{d} := {\mathbf{M_s}}^{-1}\mathbf{A_d}$$

If the scaling factors are chosen equal for all elements in $\mathbf{m}$ (i.e. for every grid block pseudopressure), the product ${\mathbf{M_s}}^{-1}\mathbf{A_d}\mathbf{M_s}$ is commutative and thus $\tilde{\mathbf{A}}_\mathbf{d} = \mathbf{A_d}$. The well index w^j is in the magnitude of 10^{-15} and may cause round-off errors in the computations. All equations involving the flow rate and thus the product of m_1 and w^j, is therefore replaced by $\tilde{w}^j\tilde{m}$ where $\tilde{w}^j := m_s w$. The rows of $\tilde{\mathbf{A}}_\mathbf{d}$ are not further scaled.

The the scaling factors in $\mathbf{M_s}$ may be chosen differently for different numerical examples of the optimization problems, mostly dependent on the time step size h. Normally, the factors are chosen in the magnitude $\sim 10^{18}$.

5.5 Alternative problem formulations

This section gives a review of alternative formulations of the optimization problem formulated in chapter 4. In particular, the potential of using only continuous variables in the problem formulation is considered.

As described in the introduction chapter, Rahmawati et al. (2009) apply a constant shut-in period to maximize the production from a *single* tight gas well. The implementation of the optimization problem is done using a high-level software integration of the reservoir model, the compressor model and the optimizer. The optimization problem is solved using a *sequential* approach with the Nelder-Mead simplex reflection method, imposing a maximum rate and a minimum rate (the minimum rate to lift) in the reservoir model and using the single shut-in time t_{SI} as optimization variable. The method is effective, but does not allow for shut-ins of variable duration. The optimizer also has little control of the simulation part, since the simulation and the optimization is done sequentially.

Adjoint-based optimization applied to petroleum reservoirs has recently generated significant interest. The application in focus has been optimal water-flooding in oil reservoirs with variations in control variables and constraints. In Zandvliet (2008) chapter 3, water-flooding in an oil reservoir model is optimized by controlling the valve settings. However, the proposed method only

considers constraints on the control input, while the computational burden for adjoint-based optimization methods are normally the presences of state constraints. The implications of state constraints are studied Suwartadi et al. (2009). Sarma et al. (2008) further address the presences of nonlinear control-sate path inequalities in adjoint models, and also gives a survey of the existing methods on these types of problems. Details of the adjoint-based optimization and the calculus of variations can be found in Bryson and Ho (1975).

The challenge of any of these methods when applied to optimization of shale gas wells, is the lower bound on the flow rate imposed as the critical rate for avoiding liquid loading. The bound

$$q(\mathbf{m}(t), \alpha(t)) \geq q_{gc}$$

will hence be an explicit input- and state constraint. The paper *Optimal Control of Switching Times in Switched Dynamical Systems* by Egerstedt et al. (2003) presents an adjoint-based optimization strategy on systems that have similarities with the problems considered in this report. The problem considers a *given* sequence of N switching times,

$$\bar{\tau} = (\tau_1, ..., \tau_N) \tag{5.24}$$

applied to the optimization problem

$$\begin{aligned} \max_{\bar{\tau}} \quad & J = \int_0^T L(x(t))dt, \\ & \text{s.t.} \\ & \dot{x}(t) = \{f_i(x(t))\}_{i=0}^N \\ & x(0) = x_0 \end{aligned}$$

where $\{f_i(x(t))\}_{i=0}^N$ is a sequence of continuously differentiable function from $\mathbb{R}^n$ to $\mathbb{R}^n$, each defined in the interval $t \in [\tau_i, \tau_{i+1})$. The paper presents a particular simple calculation of the gradient of $J(\bar{\tau})$ using an adjoint formulation, which are further embedded in the steepest decent algorithm to find the optimal switching times of the dynamical system. The assumption of continuous differentiability limits this methods applicability to the shale gas reservoir and well model developed in this report. The well performance of the shale gas well seen in figure 3.1(a) in section 3.2 has discontinuities in the derivative of the flow rate in the transition between the plateau level q_{max} and the decline rate, and when the well is shut-in. A proposal to apply the method of Egerstedt et al. (2003) on the shale gas problem is to apply

the dynamic state space model in continuous time as a sequence of switched models,

$$\dot{\mathbf{m}}(t) = \{\, \mathbf{f}_i(\mathbf{m}(t), q(t)) \,\}_{i=0}^{N} \tag{5.25}$$

and defining three different forms of the reservoir model depending on the rate:

$$\mathbf{f}_i(\mathbf{m}(t), q(t)) = \begin{cases} \mathbf{f}_{i,1}(\mathbf{m}(\mathbf{t})), & \text{if} \quad q(t) \geq q_{max} \\ \mathbf{f}_{i,2}(\mathbf{m}(\mathbf{t})), & \text{if} \quad q_{gc} < q(t) < q_{max} \\ \mathbf{f}_{i,3}(\mathbf{m}(\mathbf{t})), & \text{if} \quad q(t) \leq q_{gc} \end{cases} \tag{5.26}$$

That is, $\mathbf{f}_{i,1}$ is the right hand side (RHS) of the dynamic reservoir model with constant rate q_{max} as the applied control variable, $\mathbf{f}_{i,2}$ is the RHS of the reservoir model with the conventional well model with valve setting equal one and a constant wellhead pressure, and $\mathbf{f}_{i,3}$ is the (RHS) of the reservoir model when the well is closed, i.e. $q = 0$ [4]. In this way, a cycle of the max production, the transition region and the shut-in period is defined as *one* function that is repeated as a sequence of functions to represent the response of the reservoir model to shut-ins. To obtain continuous differentiability, the sub-functions in the piecewise function expression (5.26) may be put together using a *normalized radial basis function*. The other alternative would be to define the domain for each of the sub-functions by linear cuts and assemble the complete function (5.26) by using integer variables. However, this approach will not solve the the discontinuity problem and may not work at all.

The formulation is very experimental, and no attempt is made prove that it will work on the switching time computation of the shale gas well. The propose formulation has not been implemented in this report, and is therefore left out for further work. However, it is proposed as an *sequential* approach of solving the switching of the shale gas well, and *may* be an alternative method for solving the optimal set switchings of switchings for shale gas wells. The proposed formulation omit the discretization of state space model and have a strongly reduced number of optimization variables, while the drawback is the assumption of the known number of switchings and the need to smooth the transitions in the subfunctions (5.26).

Another algorithm for switching time computation can be found in Simakov et al. (2002). However, this algorithm also assumes a fixed number of switchings and a fixed terminal state on the time horizon of the optimization. The optimization problem may also be formulated using the continuous time ODE for the reservoir model together with the bounds on the flow rate and

[4] The bold $\mathbf{f}_i$ is used as vector notation, following the notation in the rest of the report.

the binary valve settings. The problem is then an example of mixed integer dynamic optimization (MIDO). The use of both sequential and simultaneous approaches for solving MIDO problems is described in Flores-Tlacuahuac and Biegler (2006).

Chapter 6

Results from numerical examples

This chapter presents results and analysis based of numerical examples applied to the formulations of the optimization problems in chapter 4. The optimization is performed with both single and multiple wells, and with the MINLP and MILP implementation presented in chapter 5. Unless clearly specified, the geometrical properties in table 3.1 and the reservoir and well properties in the tables 3.2 and 3.3 presented in section 3.1 will be applied in the examples.

6.1 Optimization of single well production

Two different examples are constructed to study the applicability of problem 1 in section 4.6. Both examples considers the production from a single well, and is formulated as optimization problems of short-term production planning and long-term recovery, respectively.

The properties of the gas compression are shown in table 6.1, which is used to *estimate* the cost of compressing the gas before it is sold to the market. Note the value of the inlet pressure p_c, which is set constant and low, and only used estimate of the compression cost. Note once more that possible gas fuel consumption used to produce the power to the compressor is not included in the objective function. Hence, it is assumed that all gas that is extracted from the reservoirs can be sold to the market.

The computations are performed on a Fujitsu Desktop with two 2.13 GHz processors and 16GB RAM.

Table 6.1: Compression properties

p_c	10 bar
p_m	100 bar
k_g	1.32

Table 6.2: Initial gas and power price, retrieved the 16.05.2010 from the US Energy Information Administration - EIA.

Label	Field units	SI-units	Abbreviation
G_p	5 \$/mcf	0.117 \$/ m^3	Gas price
P_p	0.0682 \$/kWh	-	Power price

Clarification: A *switching* of a well is referred to the operation of *either* closing or opening a well, that is, a shut-in *or* a re-opening.

6.1.1 Example 1: Short-term production planning of a single shale gas well

Once a shale gas well is stimulated and prepared for production, the optimal solution of problem 1 for a single will be trivial in the initial phase; As long as the flow is above the critical rate q_{gc} the optimal valve setting is to keep the well open. On the other hand, the solution is non-trivial once the rate approaches the critical rate q_{gc}.

To get a meaningful short-term optimization problem, a simulation using the base case in section 3.1 with initial pressure 200 bar is performed *prior* to the optimization. The initial grid pseudopressures of the optimization are then set equal the reservoir grid pressures from this simulation just before the flow reaches the critical rate. Precisely, the grid pseudopressures are sampled 2 years and 28 weeks after the start up of the well.

Description:

Example 1 uses the reservoir and well characteristics described base case in section 3.1, except from the initial pseudopressure as described above. Particularly, the well is assumed to operate on a constant wellhead pressure of 10 bar. The imposed minimum gas rate is the critical gas rate calculated in

section 3.4, i.e. $q_{gc} = 1.20 \cdot 10^4\,\mathrm{m}^3/\mathrm{d}$.

The time step in example 1 is set to 12 hours, thus allowing relatively frequent switching. The switching cost O_p is set to = \$200 per switching. There are no constraints on the number of switchings. Hence the function $\Psi(\eta_k^1)$ for the global switching constraints is taken out of the optimization problem. On a short-term production planning, the total operating income is considered as a better performance measure than the NPV. Hence the discount factor d_f is set to 0. The operating income is measured from initial prediction time as described above to the final prediction time T. Hence, the operating income does not included the entire life-cycle profit of the well. Example 1 is solved both with the MINLP implementation of problem 1 and with the reformulation to the MILP problem described in chapter 5.

Results:

Table 6.3: Results from *example 1* tested with different implementations and solvers. The - sign indicates that no solution is found

Prediction Time T [days]	7	14	21	28
BONMIN - GAMS				
Objective value J [\$]	9596	18275	27721	-
No. of switchings	2	8	10	-
Solution time [sec]	15.1	47.8	155.7	810
Xpress-MP - Mosel				
Objective value J[\$]	9596	19497	29265	38805
No. of switchings	2	2	2	2
Solution time [sec]	0.1	0.8	3.4	344.2
Optimality gap [%]	0.00	0.00	0.00	0.00

Table 6.3 shows the results of example 1 solved with BONMIN and Xpress-MP, respectively. The results show that the MINLP formulation solved with BONMIN finds a lower maximum objective value than the the MILP formulation solved with the Xpress-MP optimizer for two and three weeks prediction time. The solution time is clearly favorable in terms of the MILP implementation. However, the performance of BONMIN is satisfactory on small problem sets despite the discontinuity in the derivative of the extended well flow model. For a four weeks prediction time, the BONMIN does not

converge to a local feasible optimum.

Remark: In the results in both table 6.3 and 6.4, η_k is considered in the interval $k = 0, .., N-1$. Since the objective function sums the equivalent time steps, there is no cost on the last switching and the optimal solution will be to shut-in the well at the end of the prediction time, i.e. $\eta_N \equiv 1$. Hence η_N is not included in the number of switchings in the tables.

Comparison with zero switching cost:

Table 6.4 compares the solution time and the operating income for example 1 with and without the imposed cost term in the objective function, using the MILP formulation to solve the problem. To be able to compare the solutions, the operating incomes for the tests *with* the cost term are re-calculated off-line with the total switching cost removed from the objective values. [1].

Table 6.4: Comparison of the operating income for the single well in example 1 with and without a cost on the switchings. The problem is solved using the Xpress-MP Optimizer.

Prediction Time T [days]	7	14	21
Problem 1 with switching costs:			
Operating income [$]*	9996	19897	29665
No. of switchings	2	2	2
Solution time [sec]	0.1	0.8	3.4
Problem 1 without switching costs:			
Operating income [$]	9996	19943	29840
No. of switchings	2	8	18
Solution time [sec]	0.1	0.2	1.3

* The total switching cost is subtracted from J off-line after termination of the optimizer.

The difference in operating income when the switching cost is subtracted in J, is only 0.67% with three weeks prediction time. The well is switched 16 times without the switching cost and only two times with the switching

[1] In this way, the switching cost is interpreted as an imposed of "shadow" cost on the valve settings. However, it does not have the same meaning as the actual shadow price, see Williams (1993).

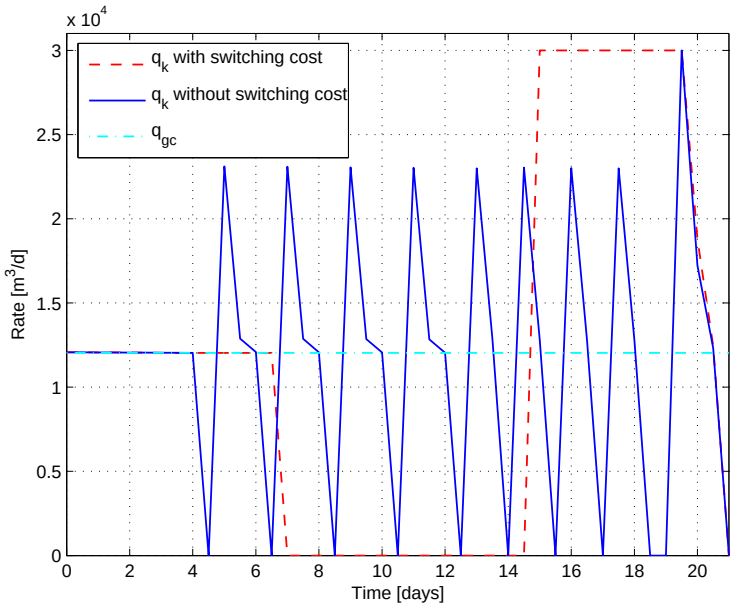

Figure 6.1: Graphical presentation of the flow rates in last column table 6.4. The subscript k only symbolizes that the values for the rates are discrete.

cost. However, the use of a cost term on the switchings is computationally demanding on the optimization algorithm, seen as an increases solution time. The optimal production plan as a result of problem 1 without a cost on the switchings, is to re-open the well once there is enough pressure to produce at a rate higher than the critical rate. This is seen in figure 6.1, where the flow rates are compared for the results in the last column in table 6.4. Without the switching cost in the problem formulation, the well is closed as short time as possible, causing many switchings with short shut-in periods. The exception is at the end of the prediction, where the well is closed for two time steps such that the well is eventually closed for $k = N$. The first switching (or shut-in) occurs earlier when there are no switching cost. In fact, the well is shut-in before the critical rate is reached with only a short shut-in period, resulting in a boost of the production rate. With the switching cost in the objective function, the well is not shut-in before strictly necessary due to the imposed minimal rate. The well stays closed longer, with a higher pressure build-up and thus a longer sustained production rate.

6.1.2 Example 2: Long term recovery of a single well

Description:

Example 2 is used to study the performance of problem 1 on a long time horizon, using the MILP formulation solved with the Xpress-MP optimizer. The well specifications are exactly the same as described in the base case in section 3.1, i.e. the initial pressure is 200 bar, the well is operating on a 10 bar constant wellhead pressure and the maximum rate is set to $3 \cdot 10^4\,\mathrm{m}^3$ per day. As in example 1, the $\Psi(\eta_k^1)$ constraint is removed from the problem formulation and the minimum rate is $q_{gc} = 1.20 \cdot 10^4\,\mathrm{m}^3/\mathrm{d}$. The fixed time step h is set to one week, the switching cost O_p is \$200 and the discount factor is 10 %. The high discount factor represents a certain risk involved with exploration of shale gas reservoirs. A one-week time step is long considering the fast dynamics in the gas reservoir. However, small time steps are generally demanding for the optimizer when using a long time horizon, and would possibly lead to termination with large duality gap.

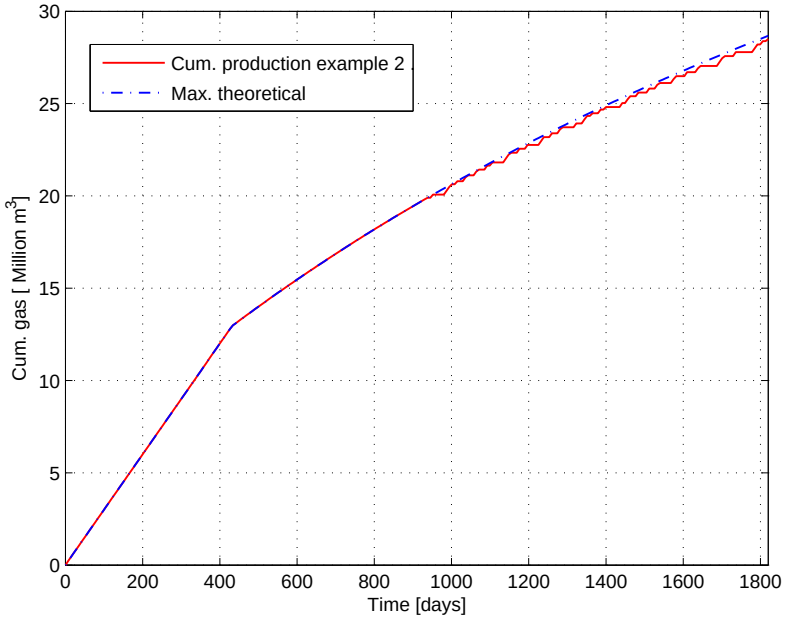

Figure 6.2: Cumulative production in example 2. The blue line is the theoretical maximum possible production if *no* liquid loading occur and the well produces continuously the entire prediction horizon.

Results:

For a five year prediction time, the optimizer is terminated after three hours, reporting the optimal NPV of 2.79 million US $. The duality gap was 0.88% when the optimizer is terminated. In figure 6.2, the cumulative production is compared with the maximum theoretical production given that no liquid loading occur and the well may produce continuously without shut-ins. Thus, the theoretical maximum does not accommodate liquid accumulation in the well. The difference in total cumulative production by using shut-ins of the well compared to a continuous production is only 0.62%. The optimal solution of example 2 yields a total of 63 switchings over five years, that is, there are 31 shut-in periods excluding the last closing of the well for $k = N$. The first shut-in is after 2.56 years. The shut-in periods spans from one to six weeks, with an average of 2.55 weeks and the median 2 weeks. No particular pattern is seen whether the long shut-in periods occur early or late in the production time after the rate for the first time falls below the critical rate.

6.2 Production optimization of multiple wells

This section presents two numerical examples on the production from multiple shale gas wells with global production constraints. Problem 1 is therefore considered with imposed global constraints in the function $\Psi(\eta_k^j)$. Once there are global production constraints on the switching capacity or requirements on the total production rate for the set of wells considered, the interactions between the wells are prominent and the optimal switching of the well is non-trivial. The two examples are on problem 1 in section 4.6.1 and on problem 2 in section 4.6.2, respectively.

Both of the next examples are solved with the MILP formulation using the Xpress-MP optimizer, as the results in the previous examples are clearly favorable in terms of this implementation. Each of the examples uses the production from **ten wells** and considers short-term production planning.

6.2.1 Example 3: Bounded total switching capacity

Description:

Example 3 is constructed to study the effect of global constraints on the switching capacity of multiple shale gas wells operated by joint administration. With a great number of wells to control and inspect, the operators will not have the capacity to switch all of the wells on and off simultaneously. The optimization problem is therefore to find an optimal distribution of the

switching capacity on the set of wells controlled.

Well specifications:

- All wells are available at initial prediction time $k = 0$. The prediction time is 2 weeks and the fixed time step h is set to 8 hours.
- All wells operate on a constant wellhead pressure set to 10 bar. The pressures of the different wells are decoupled, and the compression properties are the same as in table 6.1. Hence the estimate of the compression cost is based on the state of the gas at the wellhead pressures. The same *minimum rate* is imposed for each well, i.e. $q_{gc}^j = 1.203 \cdot 10^4\,\mathrm{m}^3/\mathrm{d}$ for all wells.
- Each well share the same reservoir properties except from the reservoir permeability and the maximum flow rate q_{max}^j. The properties are the same as in tables in section 3.1. The permeabilities are chosen randomly in an interval of $\pm 10\%$ around the reference permeability k_o=0.00075 mD. The maximum production from each well q_{max}^j is chosen similarly, with each value varying with $\pm 10\%$ around the reference value $3{\cdot}10^4\,\mathrm{m}^3$ per day. Each of the wells have been operated a given time T_p^j since last completion and the wells thus have different initial grid pseudopressures. Hence some of the wells are in the "switching-phase" while others have not been shut-in yet. The permeability, the elapsed time T_p^j and the initial state of each of the wells prior the prediction are shown in the table below.
- There are no further constraints on the number of switchings on each respective well, nor any costs on the switchings. Thus, the switching cost O_p is zero and the cost of switching the wells are instead incorporated in the constraint on the switching capacity. This is done to avoid both excessive constraints and additional costs terms on the switching variables η_k^j

* P = producing, SI = shut-in

Example 3 is implemented with two different sets of global constraints on the switching of the ten wells. This is done to compare the effects of the limited switching capacity. Thus, to distinguish between the two optimizations, example 3 is subdivided into two similar but still different optimization

Table 6.5: Example 3, well states and special properties.

Well number	1	2	3	4	5	6	7	8	9	10
T_p^j [days]	800	428	952	960	830	1210	1008	670	750	1317
k_o^j [10^{-4}mD]	7.50	7.67	7.77	7.34	7.30	8.23	6.81	8.08	8.12	7.94
q_{max}^j [10^{-4}] m^3/d	3.30	2.85	2.70	2.94	3.15	3.03	2.91	2.79	2.70	2.94
State of well*	P	P	P	SI	P	SI	P	P	P	SI

problems:

Global switching constraints in example 3a:

For the 10 wells controlled, only three switchings are allowed *per* day. Since the fixed step size is 8 hours and the prediction time is 14 days, each day consist of 3 samples. Hence the general global production constraints for the wells

$$\Psi\left(\eta_1^1, \eta_2^1, ..., \eta_k^j, ..., \eta_N^r\right) = 0$$

in problem 1 in section 4.6.1 are replaced by the set of linear constraints

$$\sum_{j=1}^{10}\left(\eta_{3l-3}^j + \eta_{3l-2}^j + \eta_{3l-1}^j\right) \leq 3, \qquad l = 1, ..., 13 \tag{6.1}$$

$$\sum_{j=1}^{10}\left(\eta_{39}^j + \eta_{40}^j + \eta_{41}^j + \eta_{42}^j\right) \leq 4 \tag{6.2}$$

The latter constraint is added to avoid that all wells are choked in the end of the prediction horizon. The choice of only three allowed switchings per day is done to enforce tight constraints; with an unconstrained number of switchings, the ten wells where switched 66 times during the same prediction time.

Global switching constraints in example 3b:

The daily constraint on the switching capacity is doubled, while the total allowed switchings over the *entire* prediction time is the same as in example 3a. The total number of allowed switchings over the entire

prediction horizon in example 3a is 43. Thus, the constraints (6.1)-(6.2) are replaced by

$$\sum_{j=1}^{10}\left(\eta_{3l-3}^{j}+\eta_{3l-2}^{j}+\eta_{3l-1}^{j}\right)\leq 6, \qquad l=1,...,13 \tag{6.3}$$

$$\sum_{j=1}^{10}\left(\eta_{39}^{j}+\eta_{40}^{j}+\eta_{41}^{j}+\eta_{42}^{j}\right)\leq 8 \tag{6.4}$$

$$\sum_{k=0}^{42}\sum_{j=1}^{10}\eta_{k}^{j}\leq 43 \tag{6.5}$$

equivalently substituted for

$$\Psi\left(\eta_{1}^{1},\eta_{2}^{1},...,\eta_{k}^{j},...,\eta_{N}^{r}\right)=0$$

in problem formulation 1. The total number of *allowed* switchings over the prediction horizon is thus identical, but the switching capacity can be shared more "freely" than in example 3a.

All other specifications are identical for example 3a and 3b. To elaborate on the ever-changing gas price, a periodic sequence of the gas price is imposed. The function is constructed by sinuous-function with one month period and an amplitude 7.5% higher than the average gas price $G_p = 5\$/\text{mcf} = 0.177\$/\,\text{m}^3$. Note that this extension of the gas price does not increase the number of variables in the optimization problem, but only affect the switching pattern of the wells.

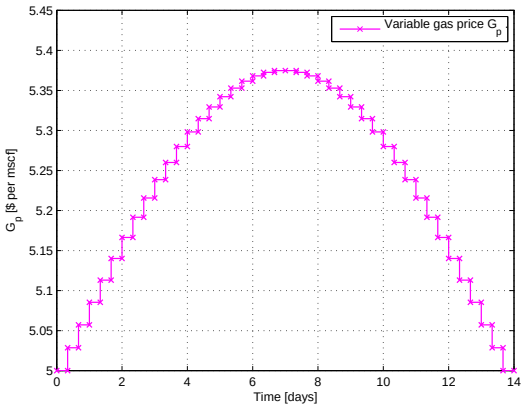

Figure 6.3: The variable gas price G_p.

Example 3b is only used as comparison with example 3a. Hence, the effects of the different well settings in table 6.5 are discussed in light of example 3a.

Results example 3a

The optimizer finds the first feasible integer solution after 22.6 minutes with a duality gap 2.6%. Although the simulation was executed for 12 hours, no more integer solutions were found and the optimality gap was only slightly reduced. The results of optimal valve settings for the ten wells over the two weeks prediction are shown in figure 6.4. The results from the optimization show that the daily maximum capacity on switchings is distributed to those wells that needs frequent switching to maintain production and at the same time are profitable for the total production. Well 4 and 10 that both are shut-in prior to the prediction, remains closed a couple more days before they are re-opened. All of the four rows in table 6.5 describing the distinct properties of the wells will affect the number of switchings for each well. Apparently, wells that have been operated a long time prior the prediction gets a higher share of the switching capacity, while wells with higher reservoir permeability are able to produce gas for a longer time once they are re-opened. A high reservoir permeability increases the conductivity in the tight shale rock that is not stimulated, thus increasing the amount of gas flowing from the outer region to the stimulated region of the reservoir during a shut-in. A figure of the flow rates can be found in appendix B.

Due to the higher permeability and maximum rate of well 6, it was expected that this well would be assigned more of the switching capacity than appearing in figure 6.4. However, as seen in figure B.1 of the well rate in appendix B, the well is actually producing on a rate just beneath the critical rate in the last phase of the prediction, even though the well appears to be shut-in in figure 6.4 above. The reason is too soft integer tolerance in the MILP solver.

Comparison of switchings in example 3a and 3b :

As seen in the comparison of the examples in figure 6.5(a), the set of wells are operated differently when the daily bound on the switching capacity is softer. In particular, the wells are switched more frequently the first three days in example 3b. In this ways, fewer shut-ins are needed during the most "profitable" time, seen as a higher sustained number of producing wells in figure 6.5(b) between day five and nine in the prediction period. In light of the gas price in figure 6.3, the wells in example 3b are more profitable during

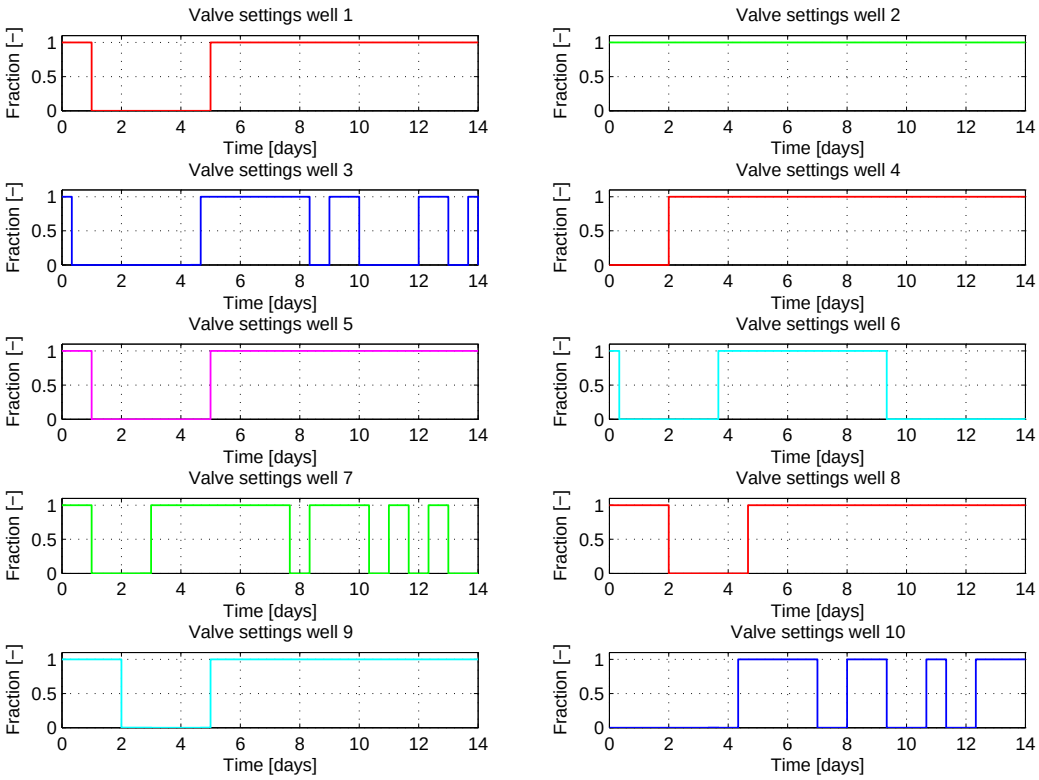

Figure 6.4: Optimal valve settings for the ten wells in example 3a.

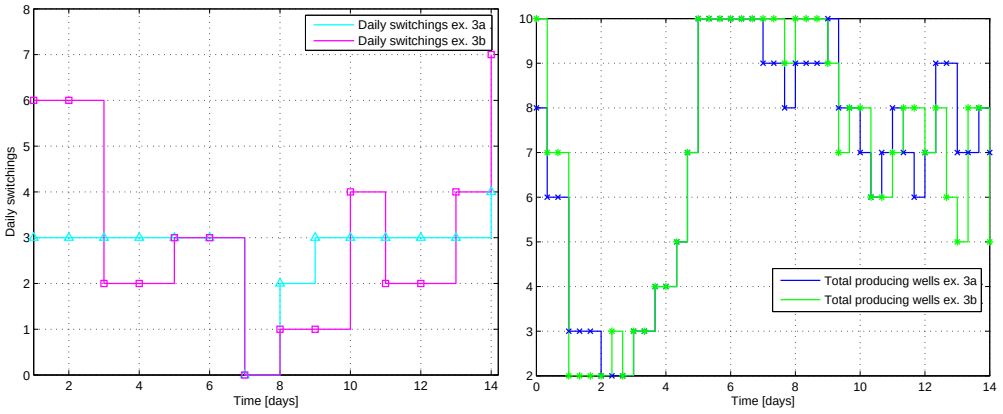

(a) Number of *daily* switchings

(b) Number of producing wells

Figure 6.5: The number of daily switchings of the wells, and the number of wells producing for the ten wells in example 3a and 3b. Note that the time axis for the left figure is counted from day 1

period with the highest gas price by lowering the production when the prices are lower. This is seen as an increased total operating income in figure 6.6.

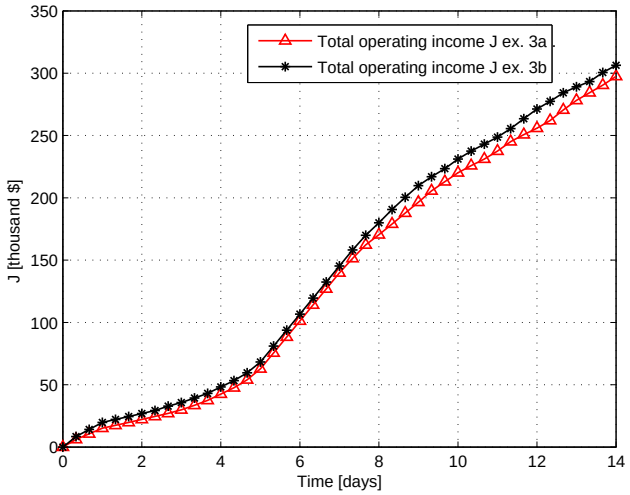

Figure 6.6: Comparison of the operating incomes in example 3a and 3b.

The total rates for example 3a and 3b are compared in figure B.2 in appendix B. The figure shows that the total rate is higher in the period *after* the peak in the gas price than before the peak, even though the price is the same. This is also seen as higher number of producing wells in this period in figure 6.5(b).

6.2.2 Example 4: Scheduling

Example 4 considers the problem of optimal scheduling of a set of shale gas wells as defined in problem 2 section 4.6.2. That is, the example considers the optimal production planning of set of wells with respect to a constant requested rate.

Description:

- The well specifications are the same as in table 6.5, used in the previous example: There are a total of 10 wells to be controlled, all wells are available at $k = 0$ and operate on a 10 bar wellhead pressure.
- The requested total rate is set to $1.80 \cdot 10^3\,\mathrm{m}^3/\mathrm{d}$, and is reformulated as the equivalent rate-per-time-step, $q_{tot,k}$, in the implementation in

Xpress-IVE. The rate is chosen reasonably with respect to the sum of the maximum possible rate from each of the wells considered.

- The optimization is done with a fixed time step $h = 8$ hour and prediction horizon is *one* week.
- There are no constraints on the switching capacity, nor any switching cost. The gas price G_p is constant 5 \$/mcf.

The penalty parameters G_1 and G_2, penalizing excessive production and too low production respectively, have a substantial impact both on the result of the optimization and the performance of the algorithm applied to this particular problem. Example 4 is therefore optimized with different values of G_1, while G_2 as shown in figure 6.7:

Red line: G_1 and G_2 are both zero.

Blue line: $G_1 = 0.5G_p$ and $G_2 = 2G_p$.

Green line: $G_1 = 2G_p$ and $G_2 = 2G_p$.

In another words, in the first optimization there is no economical loss of violating the requested rate, in the second optimization the price is halved for excessive production volumes while underproduction is penalized with twice the sales-value of the gas, and in the last optimization *both* the excessive production and the underproduction is penalized with twice the sales-value of the gas.

Results:

Figure 6.7 shows the comparison of the optimization with the different values of the penalty parameters. The production is highest with no penalties, and clearly exhibits the largest deviation from the requested rate. Penalizing both the excessive production and the underproduction equally results in the tightest production rate as seen by the green line. However, with relatively long time steps, a limited number of wells to control and only the binary valve settings as control variables, the deviation from the requested rate is still significant. With G_1 low and G_2 high, underproduction is far more expensive than the excessive production, resulting in production rates that are always as high as the requested rate if such a solution is feasible with respect to the model constraints. In this way, the loss in operating income from the rates for the red line below the requested rate is avoided as long as a feasible

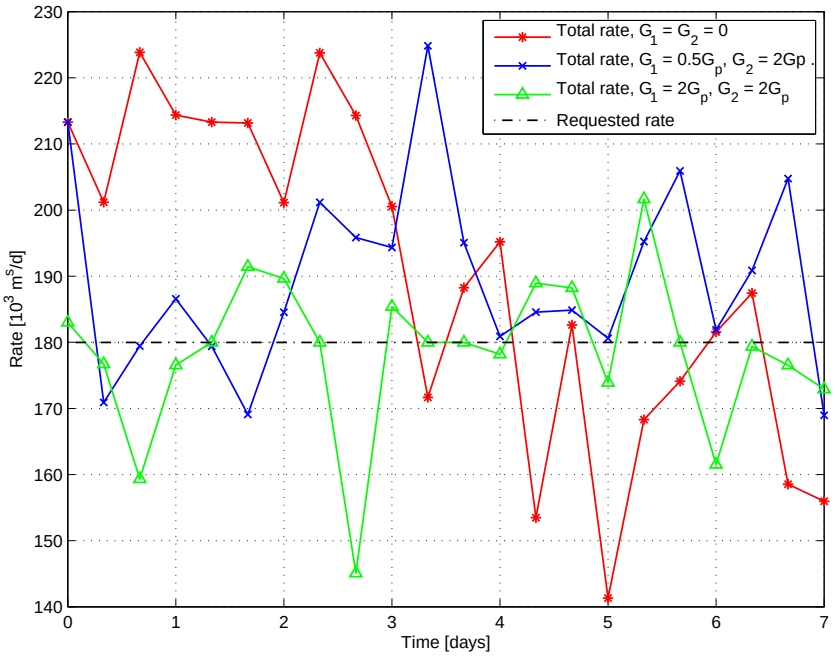

Figure 6.7: The total flow rates of the based on different penalty parameters

solution exist.

The operating income is obviously highest when there are no penalties on the excessive production and the underproduction, and lowest when there are high penalties and thus the tightest production with respect to the requested rate. The penalties on the rates result in a computationally more demanding optimization problem: With zero costs the problem terminates with zero duality gap after 72 seconds, the problem with $G_1 = 0.5G_p$ and $G_2 = 2G_p$ is terminated after 81 minutes with 2.2% duality gap while problem with equal penalties (green line) is terminated after 23 hours with 15.2% duality gap.

Chapter 7

Discussion

In this chapter, the results from the numerical examples in the previous chapter are further discussed. The advantages and the drawbacks of the different formulations and implementations are reviewed, including sources of errors on the solutions. Finally, the results are put in perspective with more practical considerations.

7.1 The different numerical examples

The main contribution in this report is the study of different problem formulations for optimal production strategy of multiple as well as single shale gas wells. In particular, the objective is to study the effects of using shut-ins with variable duration with a means to maximize the production and long-term recovery. Observations made in the results of the four numerical examples are discussed below.

Example 1 and 2:

The two examples in section 6.1 were used to study the performance of problem 1 in terms of optimization of gas production from a single shale gas well. The following observations are elaborated:

- Reformulation of the nonlinearities, constructing a MILP problem from the formulated MINLP, has great benefits both for the scalability of the optimization problems and the quality of optimal solutions. Comparing the number of switchings in the MILP and the MINLP solution in table 6.3, BONMIN "misses" the solutions with few switchings and stops the global search for the optimal solution ones it finds a locally optimum with many switchings. However, the substantial increase in the problem

size rising from the reformulation of the nonlinearities also limits the scalability of the MILP implementation.

- The switching cost decreases the number of the switchings while the shut-in period is longer. The results showed that fewer switchings of the well resulted in minimal loss of operating income. This is closer discussed below.

- On a short prediction horizon with corresponding small time steps, the optimal solution to problem 1 for a single well without any cost on the switchings will be to re-open the well as soon as possible after a shut-in. This is observed in figure 6.1. Although this *might* be an acceptable production strategy for the operation of a single well, it is not a very pronounced optimization problem.

- The NPV of a single well was successfully optimized over a prediction time of five years with varying switching periods. The total cumulative production was only reduced by 0.62% when compared to the theoretical maximum production with no shut-ins. The latter value does not accommodate the risk of liquid loading or necessary shut-ins due to maintenance, and therefore serves as the theoretical maximum without practical considerations.

Example 3 and 4:

The production environment for shale gas wells will normally consist of a substantial amount of wells located within a relatively short geographical area. From an operational perspective, the challenge will therefore be to optimally control a set of wells to meet some predefined production plan, or simply to keep the daily operating income as high as possible. At the same time, the operational capacity may be limited when there are large sets of wells to be controlled and the expenditures must be kept low to ensure the profitability of the wells.

The following observations are elaborated from the results of example 3:

- With a tight bound on the total daily switching capacity for a set of shale gas wells controlled by applying shut-ins, the result from the optimization is an optimal distribution of the switching capacity with the objective of maximizing the total operating income over the prediction time. The optimization problem is computationally demanding, and is terminated with a relatively high duality gap.

- Example 3 is solved with a varying gas price, with the result that the wells are switched optimally to produce as much gas as possible during the high peak of the gas price. If the gas price is constant, the wells might be switched differently to maximize the operating income, while the structure of the formulated optimization problem is the same. The variable gas price is used to stress more extensive switching of the wells in parts of the prediction time to maximize the production when the gas price is high.

- If the trend of the gas price can be anticipated *and* it is possible to schedule the daily operational capacity, it is beneficial to increase the man-power in part of the time to increase the number switchings, while at the same time reducing the switching capacity in other parts of the production period. This is seen as the increased the operating income for example 3b in figure 6.6.

In contrast to the other three examples which all are based on problem 1 in section 4.6.1 with different operational constraints and implementations, the last numerical example is based on *problem 2* in section 4.6.2. The following results from example 4 are emphasized:

- The penalty parameters for the excessive production and the under production, G_1 and G_2, are decisive for deviation between the actual production and the requested total production rate. In this way, the *contract* for the trade of the gas will impact the production plan. If the operator is able to sell the amount of gas produced irrespective of the deviation from the requested rate, there is no particular need to schedule the wells to produce a total specific rate. If there are great loss from too low production rates while only small loss in revenue from selling the excessive produced gas, there are benefits in terms of increased operating income obtained by optimizing the scheduling of the wells and in this way controlling the total production rate. If there are equal loss in both excessive production and under production, the results from the optimization are such that the preferred production plan is to schedule the wells with a means to produce a the total rate as close as possible to the requested rate. The different penalty parameters used in the example show how problem 2 in section 4.6.2 can be used to optimally schedule the shut-in times for a set of shale gas wells dependent on the contract for selling the gas.

- The problem of scheduling a set of shale gas wells with respect to a constant rate is a demanding optimization problem with the proposed

formulation, particular with high penalty parameters in the objective function. Optimizing the same problem over a two week prediction horizon as in example 3 was observed to be too demanding for the optimizer, and no feasible integer solution was found in the case of high values for the penalty parameters.

- Without going into details, a quadratic objective criteria might be better for the trajectory following. However, this would require a reformulation of the applied MILP formulation, and an objective function that is not formulated with respect to operating income.

7.1.1 Effects of the switching cost

The use of a switching cost decreases the number of switchings, but is at the same time computationally demanding for the optimizer. The actual costs of switching a well depends on the equipment. Modern wellhead chokes may have a fully remote control structure, thus the well can be switched from a control room and the need for on-site operator action is limited. This depends somewhat on the location of the wells and whether this kind of more expensive control equipment is installed. In this case the *actual* cost of switching the wells are minimal when employment costs are excluded in the formulation. On the other hand, any switching of the wellhead choke involve *motion* of mechanical equipment. Frequent switching of the wells will thus eventually cause tear and where on the chokes. Any mechanical motion in the wellhead chokes involves a certain risk of failure of the operation. The price of switching may therefore, to some extend, be interpreted as a risk involved with the switching. With this interpretation the switching cost should be subtracted the from the optimal objective value.

A drawback of established methods used on optimal time switching computations, is that the total number of switchings is set a priori. As stressed in Zandvliet (2008) chapter 3.5, this number is normally not known beforehand. This assumption can be omitted by using a cost on the switching as proposed in this report. However, as seen in figure 7.1, the cost must be balanced. A too high cost will "choke" the profit of the well, and consequently the number of shut-ins will be small and the duration of each shut-in long. On the other hand, a too low switching cost will diminish the effect of the cost term. Low switching costs also increases the solution of the algorithm. This is the algorithmic drawback rising from the switching cost in the objective function, also observed in table 6.4 of example 1. As comparison, by applying a maximum of *two* switchings for example 1 with zero switching costs and three weeks

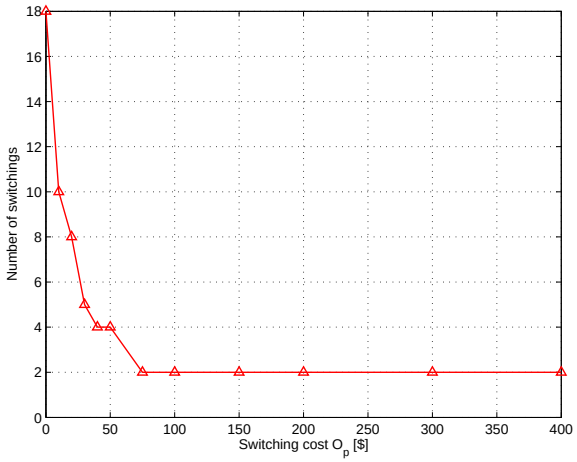

Figure 7.1: Number of switchings against the switching cost O_p, using the short term planning example 1 with three weeks prediction time. See also table 6.4

prediction time (the equivalent problem set as shown in figure 7.1 only with no switching cost), the problem is solved in 1 seconds to a optimal objective value \$29645. The corresponding problem solved with a switching cost \$200 gives an objective value \$29665 when the switching cost is subtracted as seen in table 6.4, though solved by more than three times as long solution time. The *switching times* are identical for the two problem sets, and the small difference in objective value is solely due numerical round-off errors in the optimizer, even though the optimizer options are identical. More problem is further addressed below.

As observed in table 6.4, it is possible to decrease the number of switchings without major loss of operating income. From an operational perspective, a decrease in the number of required switchings to maintain production should be an advantage even without direct costs or need for maintenance of the wells. The operation of a well will always demand surveillance by an operator, and particularly if the well is to be switched. Hence, there will always be costs associated with the daily operation and the switching of the well.

7.2 Consequences of the implementation strategy

The use of the aggregate function

Extending the conventional model of the well rate with an aggregate function, repeated here for simplicity,

$$q_k^j = \min\left\{q_{max}^j\,,\, \alpha_k^j\, w^j\left(m_{1,k}^j - m(e^s p_w^j)\right)\right\} \tag{7.1}$$

is a compensation for the lack of dynamics in the tubing modeling. However, the fact that the function is non-smooth has clear drawbacks for the optimization. Solving the MINLP implementation using BONMIN involves the use a gradient based line-search algorithm. As the derivative of (7.1) is discontinuous, the formulation is computationally demanding which in turn is reflected in the results in table 6.3. The formulation violates the assumption of twice continuously differentiable objective constraints, for which the BONMIN solver and the node NLP-solver IPOPT is designed (Bonami and Lee, 2007). Numerical issues related to ill-conditioning and insufficient scaling are also more prominent in line-search algorithms.

The cost of reformulating the expression for the well flow (7.1) is mainly due to the necessary additional binary variables $d_{1,k}$. The binary variable must be introduced for each well and for each time step, hence increasing the number of discrete variables significantly. In addition, for each well *eight* new constraints are imposed for *each* time step . In light of the above discussion, it is evidently that the problem size grows quickly with increased prediction time and additional number of wells. From the results in table 6.3, the solution time for the MILP formulation increases from 3.4 seconds to 344.2 seconds when the prediction time is increased from three to four weeks. It is hence clear that the growing problem size limits the achievable performance of the chosen implementation. However, the reformulation to a MILP problem, thereby avoiding the use of a NLP line-search algorithm to solve the relaxed problems, results in significant improvements both in the solution quality and in the performance of the optimization problems.

The simultaneous approach

The use of a simultaneous approach with full discretization of the ODE describing the reservoir model results in a large problem size. All variables including the state variables, the flow rates, the valve settings and the auxiliary variables are thus treated as optimization variables by the optimizer

(the reason for why the approach is also known as "full space"). Hence, there is no separation between the actual control variables and variables that are included in the explicit constraints describing the reservoir model. The optimal point must then be strictly feasible with respect to all of the explicit constraints describing the reservoir model, which in turn may cause feasibility problems. In dynamic optimization without discrete variables, the contrary method is known as the sequential approach (or single-shooting). Theses methods only parameterize the control variables, and thus have a strongly reduced number of variables. Two examples of this approach for implementation was described in section 5.5, both without the use of integers. These methods are generally advantageous when there are few control variables compared to many state variables, and also guarantees feasibility with the respect to the physical model. However, the sequential approach may perform worse than the simultaneous approach when there many control variables. The simultaneous approach is also advantageous for problems with state constraints (Cervantes and Biegler, 1999).

The alternative of using a sequential approach instead of the simulations approach applied in this study, can be seen in two contexts: The discretized reservoir model and the bounds on the flow rate may be re-parameterized as equivalent bounds on the discrete valve settings. This problem may be solved in a similar way as the simultaneous approach, however, with implementation of large matrices. As remarked in Diehl et al. (2009), this formulation has less structure in the linear subproblems of the optimization, and a faster local convergence is typically observed for the simultaneous approach (Diehl et al., 2009). The second context of the sequential approach is to use similar approach as formulations in 5.5, i.e. optimization without integer variables. However, the challenge involved using alternative problem formulations without the use of integer variables is caused by the minimum rate needed to prevent liquid loading, imposed as a lower bound on the nonlinear well model that can only be active when the well is producing.

There are several benefits rising from the simultaneous implementations and in particular the reformulation to a MILP problem. The simultaneous MILP implementation is very flexible. Increasing the prediction horizon or including more wells in the problem formulation is straight forward. Further, it allows for extension of the model to include for instance a variable gas or a constrained number of shut-ins for a particular well without major changes in the implementation. At last, it enables the use of powerful MILP solvers.

It is important to remark once more that the formulation of the MILP

problem is based on a *reformulation* and not a piecewise linearization of the nonlinearities in problem 1 and 2. Hence there is no loss of information involved in the reformulation, only a different way to express the flow rate in terms of additional constraints and binary variables. The possibility of reformulation instead of linearization is due to the particular simple form of the nonlinearities. Generally, this is not possible for nonlinear function, but it is an interesting feature for the type of problem considered in this report.

7.3 The duality gap

Nonconvex MINLP problems as the problems defined in section 4.6 are inherently difficult to solve. The comparison of example 1 solved with the MINLP implementation using BONMIN and the MILP implementation using Xpress-MP is clearly favorable for the MILP implementation. Although the performance of the MILP implementation decreases for large problem sets, it was chosen as the preferred solution strategy in the other numerical examples.

The duality gap defined in section 5.3 effectively computes the error bound of the optimal solution, and makes it possible to view the progress of the optimizer in real time. Figure 7.2 shows the graph in yellow of the best upper bound $\bar{J}$ of all remaining unsolved nodes, together with the best lower bound $\underline{J}$ of all solutions found so far, marked with green squares and the red line. The figure is taken directly from the Xpress-IVE interface. The solution time is shown on the lower axis and the value of the objective J on the left axis.

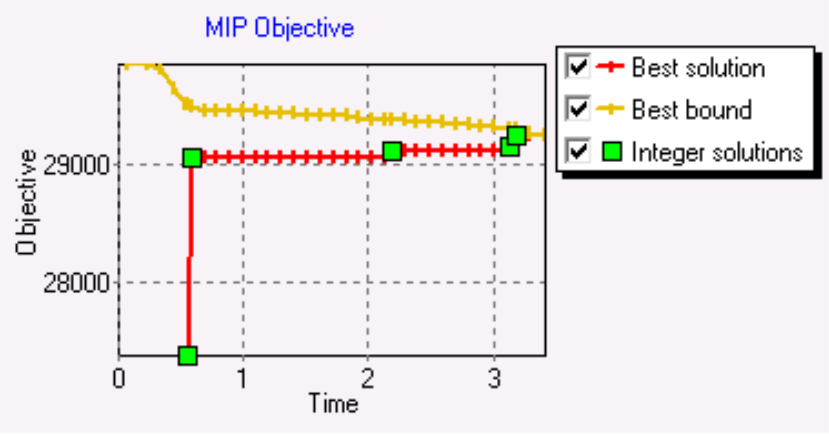

Figure 7.2: MILP duality gap from the Xpress-MP optimizer

The gap between the red and the yellow line graphically shows the duality gap and measures the relative deviation from optimality of the best feasible integer solution found so far. The particular example is the optimization of single shale gas well with three weeks prediction time and imposed switching cost. Comparing with the result in table 6.4, the algorithm terminates successfully after 3.4 seconds with less than 0.01% gap between the optimal feasible solution and the best bound.

As already mentioned, the Xpress-MP uses a duality gap less than 0.01% as default termination criteria. In several of the examples in chapter 6, the optimizer is terminated after a certain time with duality gaps larger than 0.01%. Due to the visualization duality gap, it is possible to assess the quality of the feasible solutions relative to the upper bound. Large duality gaps *may* be acceptable for some applications , and it is therefore possible to terminate the optimization at any preferred time once a feasible solution is found, still being able to quantify the optimality bound of the solution. The decrease of the upper bound is generally slow for large problem sets where the number of nodes is high.

The major difference between the solution from MILP and the MINLP formulation is the calculation of the duality gap. The solutions obtained from IPOPT of the relaxed nonconvex MINLP problem can only be guaranteed to be a locally optimal solution. The upper bound provided by IPOPT is therefore not a truly upper bound. In addition, the different starting points may result in different local optima due to nonconvexity of the problem considered. Hence the algorithm might proceed the branching on nodes that are not necessarily optimal. This is reflected in the results in table 6.3 of the comparison of the same data sets solved with BONMIN and Xpress-MP, where two of test gave a lower optimal solution when solved with BONMIN.

7.4 Numerical errors

Using a finite difference approximation of both the time derivatives as well as spatial derivatives will always introduce truncation errors. The error involved with the forward difference scheme of the radial axis decreases by choosing a finer grid, i.e. increasing N_m. This will, however, increase the size of the optimization problem, and will be detrimental for the performance of the optimizer on a large simultaneous optimization problem. More on the effects of the truncation errors can be found in Aziz and Settari (1979), and

in Knudsen (2010) for the effects on the radial composite shale gas reservoir model.

There are trade-offs between a sufficient spatial griding of the reservoir and the scalability of the optimization problem. However, with the reservoir model fixed, the time discretization will be the most dominant factor on the accuracy of the optimization.

7.4.1 The discretization scheme

Implicit Euler's method yields the least accurate implicit discretization scheme of the time axis. This choice of discretization of the prediction time therefore limits the achievable accuracy of the optimization. To quantify the resulting errors, a comparison is done by using the simulations for the base case in section 3.2, simulated using the variable step solver in Simulink as reference solution. The comparison is done without imposing the minimum rate, i.e. there is no switching of the well involved in the comparison [1]. With five years prediction time, the cumulative production of the reference Simulink solution is 29.015 million m^3.

Table 7.1: Comparison of cumulative production using implicit Euler's method (IE) for discretization of the time axis and the variable step BDF solver used in the Simulink reservoir simulation.

Time step h	Cumulative prod. IE's method [$10^6\,m^3$]	Error from reference [%]
1 week	28.673	1.18
3 days	28.617	1.37
1 day	28.588	1.47
12 hours	28.581	1.50

Table 7.1 shows that decreasing the time step actually increases the error in cumulative production when compared to the Simulink simulation with a variable step integrator. A high step size will smooth the abrupt fall in production when the production falls below the plateau rate, see figure 3.1(a)

[1] A comparison with one of the test case with several switchings is more complicated. This because the switching may be in the middle of an integration for the variable step solver, thus causing convergence issues. The comparison without switchings still give a measure of the accuracy.

and the successive discussion. The numbers in table 7.1 are therefore somewhat misleading. A shorter time step generally increases the accuracy of the model, and as seen in the numerical examples on short-term production planning, a short time step is strictly necessary to successfully optimize the switchings of the wells. On the other hand, a longer time step is necessary to enable convergence in the example on the long term recovery. Table 7.1 then shows that the error in the cumulative production in this example is reasonably low. When compared to the SENSOR reservoir model, the error will be about 8%.

Using a better discretization scheme, in particular a higher order implicit Runga-Kutta method, will increase the accuracy of the discretization. An improved discretization scheme will normally include a set of nonlinear equations that must be fulfilled for each time step. These equations may be included in the optimization problem since the reservoir model is represented as a set of equality constraints in the simulations problem formulation. However, this is not applicable for the MILP formulation without further reformulations or linearization.

The upper bound on the rate, q_{max}, prevents a high and unrealistic initial gas production. This is partly caused by the neglecting the friction term in the pressure drop in the tubing model, an assumption that may be hard to justify physically. Including the rate dependent friction term in the tubing model would form a set of nonlinear equations that must be solved for each time step by so-called nodal analysis, see for instance Guo et al. (2007) or Golan and Whitson (1991). This can straight forward be included in the MINLP model, but would not be applicable to the MILP formulation.

7.4.2 Numerical tolerances

The irregular radial grid and the composite permeability of the reservoir model results in a large spread of eigenvalues of the continuous system matrix $\bar{\mathbf{A}}$. This is recognized in the reservoir simulations by the need for an stiff numerical integrator and implicit discretization scheme of the time axis. The discretized reservoir model is thus likely to cause numerical issue for the algorithms when included as a set of equality constraints in a simultaneous optimization problem. More precisely, a set of badly scaled constraints in the optimization formulation may cause the build up of round-off errors from the finite arithmetic precision of the computer. Good scaling of the optimization problem reduces these errors. However, finding the optimal the diagonal scaling described in section 5.4 is not trivial, particularly not with the large set

of constraints resulting from the simultaneous MILP implementation. Good row scaling of the discretized state space matrix $\mathbf{A_d}$ is somewhat involved due to the large spread of the magnitude of the matrix coefficients. However, a more precise row scaling of this matrix as well as other constraints might have been beneficial for the optimizer and the reliability of the optimal solutions.

By default, the Xpress-MP optimizer uses an integer tolerance of $5 \cdot 10^{-6}$. This was observed in some cases to cause incorrect solutions for some of the binary valve settings and the respective well rates. Particularly, in figure B.1 of the well rates in example 3a it is seen that the rate for well 6 is producing at a rate just below the critical rate q_{gc}. The corresponding valve setting is close to zero, resulting in a small non-zero rates seen by the optimizer. The result is an infeasible rate that violates the imposed critical rate. In this example the integer tolerance was lowered to $2.5 \cdot 10^{-6}$. In fact, the tolerance were tightened to $1 \cdot 10^{-6}$ in a couple of the tests. This reduced the errors on the integer variables, but at the cost of substantially increased solution time and duality gaps. Actually, with too tight integer tolerance the optimizer was unable to find a feasible integer solution for example 3.

7.5 Applicability to moving horizon control

A sequence of optimal shut-in times are unlikely to be deployed in practice without any form of feedback. Gas reservoirs are generally heterogeneous, not at least because of the hydraulic fracturing, and there will always be uncertainty involved in the modeling. Even with the knowledge of certain reservoir characteristics, these are likely to change during the life-cycle of a shale gas well, thus requiring model update. In light of the risk of liquid loading in the wells, sudden shut-ins of some of the wells may occur and the surface facilities may fail. This will change the production settings, requiring updates and re-optimization of the production planning. Hence long-term prediction of optimal switching times of a well are most useful to study the *potential* profit of a well, while the practical applicability of the optimal solution are rather limited.

A possible implementation strategy would be to use *moving horizon control*. For a given prediction time and sampling interval, only the first optimal valve-settings α_1^j would be applied the set of wells controlled before a re-optimization is performed with updates from both measurements and the

inputs of the system. The full state vector of the grid pseudopressures must be available in order to apply any of the proposed optimization formulations in practice. These are obviously not measurable states. Hence, there will be a need for state estimation, typically a form of the Kalman filter. The use of model-based production optimization in practice also put requirements on the instrumentation. In particular, a measure of the pressure differential over the wellhead choke is necessary to include the flow rates in the calculations.

The very brief discussion on moving horizon control stops here, and is only included with a means of putting the optimization problems into a larger control perspective. However, the above section is also a proposal for further work on the control of shale gas wells.

7.6 Production optimization in practice

The results obtained from numerical optimization of the production planning must always be put in perspective with operational requirements for a production plant. Operational challenges often extends far beyond what is included or even can be included in an formulation of a mathematical optimization problem.

The production planing of today's shale gas plays is typically based on the operators experience and knowledge of the production profile of shale gas wells. On-site decision making may be based on available real-time information of the production, as well as the production history of the wells. Operators will often monitor a set of wells, and try to either meet the goals of a given production plan or simply to produce as much gas as possible. As a first step to actually employing model-based production optimization of shale gas wells, one possibility would be to provide the operators with a sort of production plan for a set of wells, typically for a couple of days or up to a week. There more or less always constraints in the production capacity. These constraints may for instance be constraints in the switching capacity of the wells or a request for a certain total gas rate, thus in resemblance with the examples in chapter 6. A production plan can then be formulated by support of the proposed optimization problems and implementations done in this report. If one well is producing without the need for shut-ins, this well may be left out while optimizing the switching capacity on the rest of the controlled wells by using one of the proposed optimization problems. In this way, the model-based optimization of shale gas wells may be used as a decision *support* for the operator. By the results in example 2 on long-term gas

recovery, the model-based optimization may also be applied with the means of decision support for planning, commissioning and drilling of new shale gas wells.

The gas price will naturally affect production planning, both on short-term and long term production planning. The gas price is generally volatile and can be difficult to predict. However, based on historical data and known seasonal variations in the demand for natural gas, it is to some extend possible to predict the gas price. See for instance Reiter and Economides (1999). In such manner, the production plan of shale gas wells may be supported by the proposed optimization formulation as seen in example 3 in section 6.2.1. The development of the gas price in the United States is included in figure 7.6.

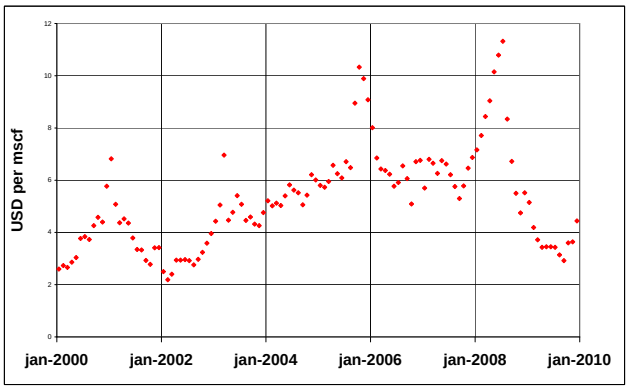

Figure 7.3: US wellhead gas price in monthly intervals since 2000. Source: US-EIA

The use of shut-ins for boosting the production is both unlikely and not intended to replace the use of multistage hydraulic fracturing. This stimulation technique is essential for the production, and is together with drilling of horizontal wells the most important factor for the improvement seen the last decade in the productivity of shale gas wells. However, the use of hydraulic fracturing on a regular basis is both expensive and depends on the availability of large quantities of water. The use of shut-ins of shale gas wells may therefore be used as a cost-saving *supplement* to the stimulation with hydraulic fracturing.

Chapter 8

Conclusion

The main contribution of this thesis is the development and study of model-based optimization applied to shale gas wells. The formulated production optimization problems are special in terms of using the simultaneous approach with binary variables for modeling on/off valves. The reformulation from a MINLP problem to a MILP problem, is shown by numerical examples to improve the solution quality and reduce the solution time. On the other hand, it is observed that both the simultaneous approach and the use of binary variables limits the scalability of the optimization problems.

By four numerical examples, it is shown how the use of shut-ins can be applied as a means of boosting the production and preventing liquid loading in shale gas wells. The long-term recovery for single shale gas well was optimized using shut-ins with variable duration and observed to result in only small losses of cumulative production compared to the theoretical possible maximum rate. In terms of short-term production planning, it is possible to reduce the number of switchings of a well without substantial loss in operating income. For production from multiple shale gas wells with global production constraints in switching capacity or production rate, the implemented optimization problems show how shut-ins of the wells can be applied to increase the profit due to varying gas prices and sales-contracts.

The reservoir model and production setting developed and integrated in the model-based optimization in this thesis are simplifications of the real production system for shale gas wells. More accurate representation of the models and the production settings are needed in order to apply the proposed optimized production strategies in practice. However, the results show a significant potential of using shut-ins to plan and boost the production from shale gas wells.

Chapter 9

Further work

The limitations seen on the scalability of the proposed problem formulation, motivates the use of parallel computations when solving the optimization problem. The use of parallel computations in mathematical optimization is a major research area, and makes it possible to solve a majority of problems that up to this date have been too big for the existing computation resources. As the inter-dependencies between the wells in the model formulation are minimal, the use of efficient decomposition algorithms may be possible, thus allowing parallel computations. In this way, the original optimization problem may be solved as subproblems, defined with the objective of maximizing some asset of the large group of wells. This may allow for a site-wide production optimization of shale gas plays, which is, considering the fact that some plays have hundreds or even thousand producing wells, a very challenging optimization problem. The use of decomposition algorithms applied to petroleum production systems are studied in Gunnerud and Foss (2009).

Several improvements in terms of the modeling and the formulation of the optimization problems may be applied. The system of the wells may be imposed a tighter coupling scheme in the optimization problem by including an improved compression model and surface pressure calculations of the different wells. An improvement on the modeling, would be to use a multi-layered horizontal well model. This will significantly improve to realism in the rate predictions, but at the cost of a numerically more demanding reservoir model.

Including the optimization problems in a closed-loop reservoir management or a moving horizon control is also proposed as possible further work.

List of symbols

Nomenclature

c	total gas compressibility, 1/Pa
g	gravity, m/s^2
G	gas gravity, dimensionless
h	reservoir thickness, m
k	permeability, mD
k_g	gas specific heat ratio, dimensionless
M	molecular mass of the gas, kg/mol
m	pseudopressure, Pa/s
m_i	initial reservoir pseudopressure, Pa/s
m_{wf}	well bottomhole pseudopressure, Pa/s
p	reservoir grid pressures, bar
p_c	compressor inlet pressure, bar
p_{init}	initial reservoir pressure
p_w	wellhead pressure
p_{wf}	well bottomhole pressure, bar
q	well flow rate, m^3/s
R	universal gas constant, 8.3145 J/Kmol
T	reservoir temperature, K
z_w	well height, m
Z	gas compressibility factor, dimensionless
μ	viscosity, Pa·s
ρ	gas density, kg/m^3
ϕ	reservoir porosity, dimensionless

Subscripts

c	compressor
d	discrete representation
g	gas
gc	gas critical rate
sc	standard conditions, 1 bar and 15.5°C
w	evaluation at wellhead condition

Abbreviations

BVP	boundary value problem
GAMS	General algebraic modelling system
IE	Implicit Euler's method
IPR	inflow performance relationship
IVP	intial value problem
LP	linear program
LR	linear relaxation
LTI	linear time-invariant
MILP	mixed integer *linear* program
MINLP	mixed integer *nonlinear* program
NLP	nonlinear program

Bibliography

Abou-Kassem, J. H., Ali, S. F., and Islam, M. R. (2006). *Petroleum Reservoir Simulation, A Basic Approach*. Gulf Publishing Company.

Al-Ahmadi, H. A., Almarzooq, A. M., and Wattenbarger, R. (2010). Application of linear flow analysis to shale gas wells - field cases. In *SPE 130370, Unconventional Gas Conference*, Pennsylvania, USA.

Al-Hussainy, R., Jr., H. R., and Crawford, P. (1966). The flow of real gases through porous media. *Journal of Petroleum Technology*, 18(5):624–636.

Arthur, J., Bohm, B., and Layne, M. (2008). Hydraulic fracturing for natural gas well of the marcellus shale. In *The Ground Water Protection Council 2008 Annual Forum*, Ohio.

Aziz, K. and Settari, A. (1979). *Petroleum Reservoir Simulation*. Applied Science Publishers Ltd.

Bieker, H., Slupphaug, O., and Johansen, T. (2006). Real time production optimization of offshore oil and gas production systems: A technology survey. In *SPE 99446, Intelligent Energy Conference and Exhibition*, Amsterdam, The Netherlands.

Bonami, P., Biegler, L. T., Conn, A. R., Cornuéjols, G., Grossmann, I. E., Laird, C. D., Lee, J., Lodi, A., Margot, F., Sawaya, N., and Wächter, A. (2008). An algorithmic framework for convex mixed integer nonlinear programs. *Discrete Optimization*, 5:186–204.

Bonami, P. and Lee, J. (2007). *BONMIN User's Manual*. COIN-OR.

Bryson, A. E. and Ho, Y.-C. (1975). *Applied Optimal Control*. John Wiley & Sons.

Carlson, E. (1994). Characterization of devonian shale gas reservoirs using coordinated single well analytical models. In *SPE 29199, Eastern Regional Meeting*, West Verginia.

Carlson, E. and Mercer, J. (1991). Devonian shale gas production: Mechanisms and simple models. *SPE 19311-PA, Journal of Petroleum Technology*, 43(4):476–482.

Cervantes, A. and Biegler, L. (1999). Optimization strategies for dynamic systems. In *In C. Floudas, P. Pardalos (Eds), Encyclopedia of Optimization*. Kluwer Academic Publishers.

Chen, C.-T. (1999). *Linear System Theory and Design*. Oxford University Press.

Cipolla, C., Lolon, E., and Mayerhofer, M. (2009). Reservoir modeling and production evaluation in shale-gas reservoirs. In *International Petroleum Technology Conference*, Doha, Qatar.

Cipolla, G. L. (2009). Modeling production and evaluating fracture performance in unconventional gas reservoirs. *Journal of Petroleum Technology*, 61(9):84–90.

Diehl, M., Ferreau, H. J., and Haverbeke, N. (2009). Efficient numerical methods for nonlinear mpc and moving horizon estimation. *Nonlinear Model Predictive Control, LNCIS*, 384:391–417.

Egeland, O. and Gravdahl, J. T. (2003). *Modelling and Simulation for Automatic Control*. Tapir Trykkeri.

Egerstedt, M., Wardi, Y., and Delmotte, F. (2003). Optimal control of switching times in switched dynamical systems. In *IEEE Conference on Decision and Control*.

Elmer, W. G., Elmer, S. J., and Elmer, T. E. (2009). New single well standalone gas lift process facilitates barnett shale fracture treatment flowback. In *SPE 118876-MS, Production and Operations Symposium*, Oklahoma.

FICO^{TM}(2009). Mip formulations and linearizations. Xpress Optimization Suite Documentation.

Flores-Tlacuahuac, A. and Biegler, L. T. (2006). Simultaneous mixed-integer dynamic optimization for integrated design and control. *Computers and Chemical Engineering*, 31:588 – 600.

Golan, M. and Whitson, C. (1991). *Well Performance*. Prentice Hall, 2nd edition.

Gunnerud, V. and Foss, B. (2009). Oil production optimization − a piecewise linear model, solved with two decomposition strategies. *Computers and Chemical Engineering*, doi:10.1016/j.compchemeng.2009.10.019.

Guo, B., Lyons, W. C., and Ghalambor, A. (2007). *Petroleum Production Engineering, A Computer-Assisted Approach*. Gulf Professional Publishing.

Jenkins, C. D. and Boyer II, C. M. (2008). Coalbed- and shale-gas reservoirs. *Journal of Petroleum Technology*, 60(2).

J.H. Frantz, Jr., Williamson, J., Sawyer, W., Johnston, D., Waters, G., Moore, L., MacDonald, R., Pearcy, M., Ganpule, S., and March, K. (2005). Evaluating barnett shale production performance using an integrated approach. In *SPE Annual Technical Conference and Exhibition*, Texas.

Katz, D. L. and Lee, R. L. (1990). *Natural Gas Engineering*. McGraw-Hill Publishing Company.

Knudsen, B. R. (2010). Modelling and simulation of shale gas reservoirs. 9th semester project report, Norwegian University of Technology and Science.

Li, M., Sun, L., and Li, S. (2001). New view on continuous-removal liquids from gas wells. In *SPE 75455, Permian Basin Oil and Gas Recovery Conference*.

Medeiros, F., Ozkan, E., and Kazemi, H. (2007). Productivity and drainage area of fractured horizontal wells in tight gas reservoirs. In *Rocky Mountain Oil and Gas Technology Symposium*.

Nocedal, J. and Wright, S. J. (1998). *Numerical Optimization*. Springer Verlag.

North, F. K. (1990). *Petroleum geology*. Chapman & Hall.

Petroleum Experts Ltd. (2008). Turner equation. Prosper version 10.4 Reference Manual.

Pochet, Y. and Wolsey, L. A. (2006). *Production Planning by Mixed Integer Programming*, volume Springer Series in Operations Research and Financial Engineering. Springer.

Rahmawati, S., Whitson, C. H., and Foss, B. (2009). New optimal strategy for stranded tight-gas reservoirs. In *Seminar on Stranded Gas Including Low Permeability Reservoirs, Yogyakarta, Indonesia*.

Reiter, D. F. and Economides, M. J. (1999). Prediction of short-term natural gas prices using econometric and neural network models. In *SPE 52960-MS, Hydrocarbon Economics and Evaluation Symposium*, Dallas.

Sarma, P., Chen, W. H., Durlofsky, L. J., and Aziz, K. (2008). Production optimization with adjoint models under nonlinear control-state path inequality constraints. *SPE Reservoir Evaluation and Engineering*, 11(2):326–339.

Schettler, P., Parmely, C., and Lee, W. (1989). Gas storage and transport in devonian shales. *SPE Formation Evaluation*, 4(3):371–376.

Simakov, S. T., Kaya, C. Y., and Lucas, S. K. (2002). Computations for time-optimal bang-bang control using a lagrangian formulation. In *Preprints of the 15th World Congress of IFAC*, Barcelona, Spain.

Smith, T. (2007). Producing gas from shales. `http://www.geoexpro.com/sfiles/4/13/5/file/gasfromshales.pdf`. GEO ExPro, p.49.

Suwartadi, E., Krogstad, S., and Foss, B. (2009). On state constraints of adjoint optimization in oil reservoir water-flooding. In *SPE 125557, Reservoir Characterization and Simulation Conference*, Abu Dhabi.

Turner, R., Hubbard, M., and Dukler, A. (1969). Analysis and prediction of minimum flow rate for the continuous removal of liquids from gas wells. *Journal of Petroleum Technology*, 21(11).

Verdult, V. and Verhaegen, M. (2000). Bilinear state space systems for nonlinear dynamical modelling. *Theory in Biosciences*, 119.

Warren, J. and Root, P. (1963). The behavior of naturally fractured reservoirs. *SPE Journal*.

WEO (2009). *World Energy Outlook 2009 - Prospects for Natural Gas*, chapter 11. International Energy Agency.

Williams, H. P. (1993). *Model Building in Mathematical Programming*. John Wiley & Sons.

Wolsey, L. A. (1998). *Integer Programming*. John Wiley & Sons, Inc.

Zandvliet, M. J. (2008). *Model-based Lifecycle Optimization of Well Locations and Production Settings in Petroleum Reservoirs*. PhD thesis, Technische Universiteit Delft.

Appendix A

Gas properties

The calculation of the gas properties is based on a gas gravity $G = 0.7$ and reservoir temperature $T = 366.3$ K. The Z-values are based on Hall & Yarbourough correlation and the μ-values are based on Lee-Gonzales correlation (courtesy of Professor C.H. Whitson).

Table A.1: Gas properties

p [10^5 Pa]	Z [-]	μ [10^{-3} Pa $\cdot$ s]
10	0.9872	0.0131
20	0.9748	0.0133
30	0.9629	0.0135
40	0.9516	0.0137
50	0.9408	0.0139
75	0.9168	0.0147
100	0.8976	0.0155
125	0.8842	0.0165
150	0.8772	0.0177
175	0.8768	0.0189
200	0.8825	0.0202
225	0.8939	0.0216
250	0.9100	0.0229
275	0.9299	0.0243
300	0.9528	0.0256
325	0.9780	0.0269
350	1.0051	0.0281

Appendix B

Additional plots

Figure B.1 shows flow rates from the ten wells in example 3a section 6.2.1. The problem with insufficient tolerance on the binary variables are reflected in flow rate for well 6, which is treated as zero by the optimizer but results in a value just beneath the critical rate when re-scaled to actual values.

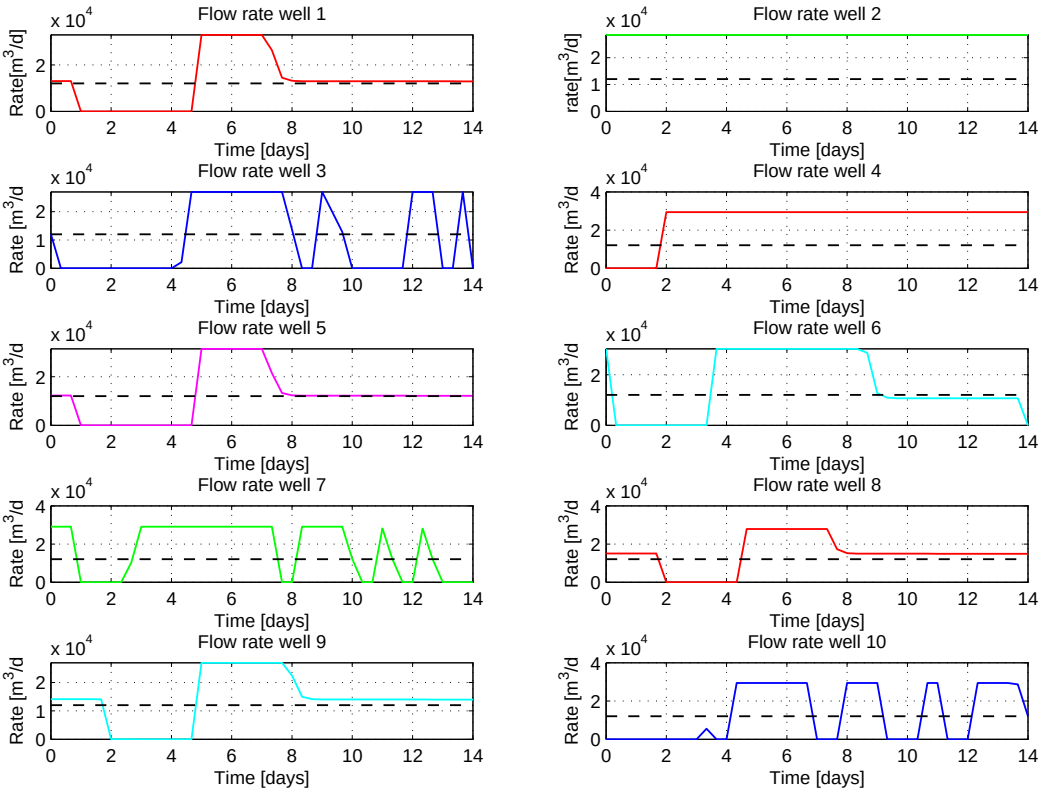

Figure B.1: The ten flow rates in example 3a.

Figure B.2 shows the total rates for the ten wells in example 3a and 3b, producing with tight bound on the daily switching capacity and soft bound in addition to a total bound on the swithcing capacity, respectively.

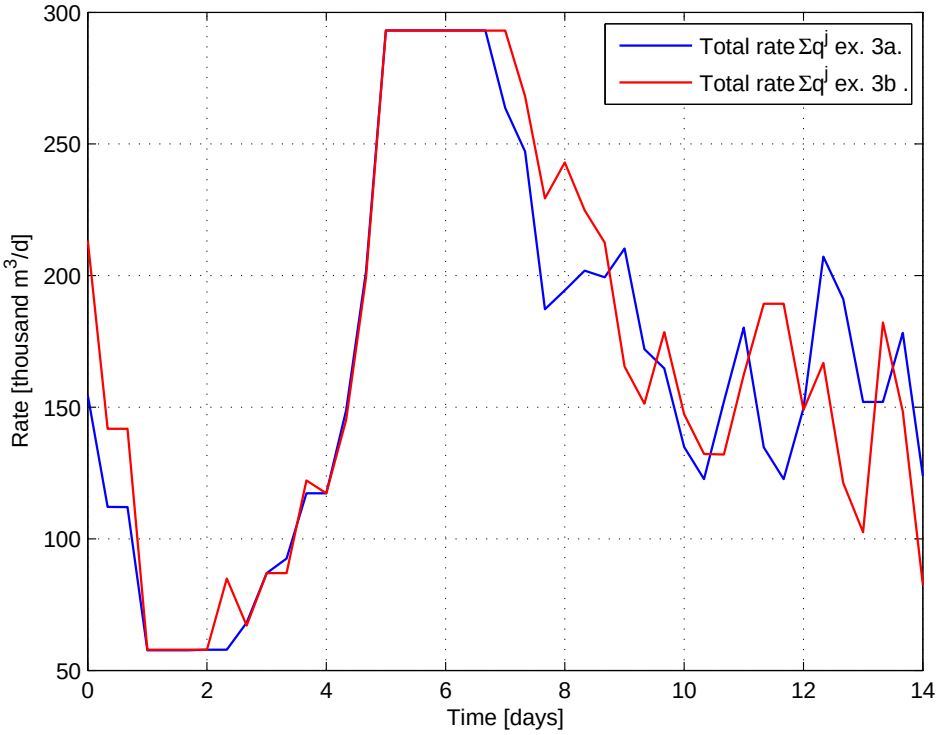

Figure B.2: Comparison of the total rates in example 3a and 3b.